13798 A

(AR 530-1, Operations Security)

I am aware that there is foreign intelligence interest in open source publications. I have sufficient technical expertise in the subject matter of this paper to make a determination that the net benefit of this public release outweighs any potential damage.

Reviewer: LISA PROKURAT FRANKS (Name) GS13 (Grade) Materials Engineer (Title)

[signature] (Signature) 12 JUN 01 (Date)

Description of Information Reviewed:

Title: Explosively Bonded Armor Materials

Author/Originator(s): John Krebsbach and Ina Krebsbach (Editor)

Publication/Presentation/Release Date: 13 Aug 96

Purpose of Release: Submission of technical report

An abstract, summary, or copy of the information reviewed is available for review.

Reviewer's Determination (circle one):

(1) Unclassified Unlimited.

2. Unclassified Limited, Dissemination Restrictions IAW _____.

3. Classified. Cannot be released, and requires classification and control at the level of _____.

Security Office (AMSTA-CS-S):

(Concur)/Nonconcur [signature] (Signature) 18 JUN 01 (Date)

Public Affairs Office (AMSTA-CS-CT):

(Concur)/Nonconcur Margaret Compton (Signature) July 12, 2001 (Date)

20011108 039

REPORT DOCUMENTATION PAGE

Form Approved
OMB No. 074-0188

1. AGENCY USE ONLY (Leave blank)	2. REPORT DATE	3. REPORT TYPE AND DATES COVERED
	13Aug96	Final, 30Mar97 - 30Sept99

4. TITLE AND SUBTITLE
Explosively Bonded Armor Materials

5. FUNDING NUMBERS
SBIR Topic A95-015, Phase II

6. AUTHOR(S)
John Krebsbach
Ina Krebsbach (Editor)

7. PERFORMING ORGANIZATION NAME(S) AND ADDRESS(ES)
Adaptive Coating Technologies, LLC
4836 Morris Court
Waunakee, WI 53597

8. PERFORMING ORGANIZATION REPORT NUMBER
sb95015 (13798A)

9. SPONSORING / MONITORING AGENCY NAME(S) AND ADDRESS(ES)
TACOM
AMSTA-AQ-WAA
Marlene Ross
Warren, MI 48397-5000

10. SPONSORING / MONITORING AGENCY REPORT NUMBER
DAAE07-97-C-X049

11. SUPPLEMENTARY NOTES

12a. DISTRIBUTION / AVAILABILITY STATEMENT
Public information

12b. DISTRIBUTION CODE

13. ABSTRACT ***(Maximum 200 Words)***

A unique method of fabricating armor plate has been demonstrated. The process produces an extremely hard steel/titanium composite material. Patent is pending.

14. SUBJECT TERMS
Bond, Armor, Plate, Explosive bonding, Titanium, Tool steel

15. NUMBER OF PAGES
56

16. PRICE CODE

17. SECURITY CLASSIFICATION OF REPORT	18. SECURITY CLASSIFICATION OF THIS PAGE	19. SECURITY CLASSIFICATION OF ABSTRACT	20. LIMITATION OF ABSTRACT
Unclassified	Unclassified	Unclassified	

Adaptive Coating Technologies, LLC

315 Raemisch Rd., Building H
Waunakee, WI 53597

Technical Report for SBIR Topic # A95-015, Phase II

Proposal Title: Explosively Bonded Armor Materials

Period Covered: March 30, 1997 Through September 30, 1999

DOD Contract #**DAAE07-97-C-X049**
Contract Data Requirements List, Data Item A002, Final Report
Unclassified Document
Unlimited Distribution

TACOM
Warren, MI 48397-5000
Date: November 15, 1999

Table of Contents

Section		Page
5.	Ballistic Simulation Modeling	24
6.	Residual Stress Data	24-26
7.	Other	26
8.	Conclusion	26
III.	**References**	**26-27**

Tables

Photos

Section Page

Figures

I. Phase II Project

A. Introduction

Ultra high hardness steel is often used as an economical armor material, but its use as a structural material is limited because of its low ductility, high hardness, and difficulty in welding and machining. Titanium, however, with its high strength-to-weight ratio, is a good structural material with relatively high ballistic performance. Coupling titanium with an ultra high hardness steel could utilize the strengths of both materials and may provide an economical alternative for certain light armor applications, such as the light armor vehicle (LAV).

Conventional welding of either titanium or high hardness steels presents various problems. For example, welding high hardness steels (i.e. Rockwell C60 minimum) demands careful attention because of the material's low ductility and extreme crack sensitivity. Dramatic microstructural differences among the weld metal, heat affected zone and steel base metal exist. These variances result in substantial ductility, hardness and strength differences, which may cause failure at the joint region. As a result, post heat treatments are usually required to relieve the material stresses. In addition, titanium requires special gas shielding techniques during welding to prevent surface oxidation. Using conventional welding processes to overlay titanium onto high hardness steels, or visa versa, would involve not only the problems previously mentioned but also the formation of various brittle intermetallics at the titanium-steel interface. The conventional welding processes, therefore, are highly impractical for attaining an adequate, cost effective titanium-steel bond.

Explosive bonding, however, could be more pragmatic, as it offers several advantages over the conventional welding processes for bonding titanium and steel. Explosive bonding of two materials generates an interface morphology that has minimal microstructural changes in the flyer and backer plates. Dilution between the two materials is minimized, and therefore brittle intermetallics, if present, are isolated and surrounded by ductile metal. Also with explosive bonding, the oxide layer of a material like titanium is removed just prior to bonding. Reduced wetting, along with the intimate contact formed between the two unoxidized metals during explosive bonding, should produce a joint with high adhesive strength.

Commercial explosive bonding of titanium flyer and steel backer plates uses steel with a surface hardness less than Rockwell C45 and a yield strength less than 100,000 psi. However, when backer materials have a hardness and yield strength above these values, as is the case with ultra high hardness steel substrates, explosive bonding is difficult even with the use of a low yield strength thin interlayer material. Therefore annealed steel and titanium materials were used for the explosive bonding work.

After explosive bonding of the dissimilar materials, the steel material attains a hardness value of only Rockwell C22. Consequently post heat treatment is necessary to bring the material up to the required hardness and produce the martensitic formation. Commercial

heat treating methods generally involve slow heating rates and long soak times, and therefore create additional undesired diffusion at the titanium/iron interface. The infrared heating method used for this work is more versatile, with several advantages over conventional localized heating technologies. The infrared heating process has a higher heating rate and lower soak times, which minimizes undesired interfacial diffusion. In addition its directional heating capability reduces stress due to thermal expansion differences in the two dissimilar materials. Also it minimizes oxygen contamination of the titanium surfaces during heating while still allowing the composite material to be water or oil quenched, which produces good hardness of the steel material.

Results indicate that although tool steel and Hi-hard composite plates can be explosively bonded and subsequently heat treated, the Hi-hard/Ti-6-4 combination should be the composite on which to concentrate for the following reasons. First, the difference in physical properties between the various tool steels and titanium is much greater than between hi-hard and the titanium materials (i.e. ductility, thermal expansion, etc.). Second, bend testing conducted with hardened Hi-hard material exhibited higher ductility than the tool steel materials. Third, computer modeling of ballistic testing with Hi-hard/Ti-6-4 composite material indicates good results with M2AP projectiles at 2500+ fps velocities. And last, the U.S. military has extensive data on the use of high-hard as armor material. Therefore the final plates submitted for ballistic testing are Hi-hard/Ti-6-4.

In conclusion, this project has produced more lightweight and ballistically superior armor than conventional armor systems. The Ti-6-4/RHA composite steel plates are not only hard but also capable of withstanding repeated ballistic hits with M2AP projectiles without plate fracture or complete joint delamination.

Also, an even more advanced armor can be achieved in the future by using thin interlayer materials to substantially reduce the intermetallics at the bond interface, which subsequently increases bond strength and joint ductility. Anticipated benefits include better ballistic performance and plates that may be easily straightened with a hydraulic press. Maximum armor fabrication dimensions were previously 8" x 8", but recent discoveries make it possible to produce these more advanced armor plates a minimum of 12" x 12".

B. Summary

Scope of Work

The following scope of work was detailed in DOD Contract #DAAE07-97-C-X049:

1.1 The Contractor, acting as an independent Contractor and not as an agent of the Government, shall provide the necessary personnel, facilities, materials, and services to develop hard faced armors with ductile titanium and titanium alloy backing to improve both ballistic performance and systems integration. The effort shall continue work

explored and completed under the Phase I SBIR, Topic A95-015, Explosive Bonding of Titanium and Alloyed Steel.

1.2 The Contractor shall develop the parameters to explosively bond and subsequently heat treat Titanium (Grade 2) and Ti-6Al-4V backing plates to various tool steels to include A2, D2, and M2 steels. Samples shall be prepared using 15" x 15" materials nominally .25" in thickness (a resulting bonded sample of .5" in thickness).

1.3 The Contractor shall evaluate the bonded materials to determine bond joint integrity and quality using both destructive and non-destructive inspection techniques.

1.4 The Contractor shall develop the parameters to explosively bond and subsequently heat treat the bonded samples to establish the maximum steel component hardness while maintaining a high quality bond and minimizing the heat effect on the titanium component.

1.5 The Contractor shall evaluate the heat treated materials to determine bond joint integrity and quality, steel component properties, and backing component properties using both destructive and non-destructive inspection techniques.

1.6 The Contractor shall prepare and submit six (6) ballistic samples (12" x 12") for evaluation by the Government for each tool steel and titanium combination.

1.7 The Contractor shall evaluate the results of sample development with 15" x 15" materials to select final titanium alloy for bonding, heat treatment and evaluation of 30" x 30" samples of A2, D2, and M2 tool steels. Six (6) ballistic samples (24" x 24") shall be prepared for evaluation by the Government.

1.8 The Contractor shall survey alternative bonding techniques and evaluate one alternative bonding method to develop samples for physical and metallurgical testing.

Contract Changes

The scope of work requirements were completed except for the following changes:

- 15" x 15" A2 and D2 tool steel composite plates were produced; however the joint ductility appeared inadequate for ballistic testing irregardless of the titanium material component. Hi-hard composite plates were also produced and were submitted for ballistic testing. M2 tool steel was not a viable steel material due to the high austenitizing temperature required during the hardening process.
- Some of the plates were dimensionally larger or smaller than the proposed 12" x 12" because of deviations in the explosive bonding process that resulted in unbonded regions of varying sizes around the plate perimeter.

- Ballistic impact computer modeling was implemented to predict the performance of the various steel and titanium composites
- The final plate dimensions submitted for ballistic testing were changed to 15" x 15" due to the size limitations of the heat treat equipment.

Future Project Investigations For Improved Ballistic Performance:

- Apply a thin film interlayer to the steel component prior to explosive bonding for elimination of the brittle intermetallic formation.
- Adjust the explosive bonding setup to produce a flatter composite plate.
- Investigate vacuum hardening processes for the heat treating setup that tolerate varying amounts of plate distortion

Ballistic Test Results

The tail ballistic test data sheet from the three Phase I 12" x 12" A2/Ti plates is shown in Table 1. All three composite plates withstood one ballistic hit, but with the second hit, they either partially or totally delaminated at the interface. Visual examination of all ballistically damaged areas shows that the interior surfaces of the tool steel have a conical shape, which indicates a brittle fracture and a material that absorbs little kinetic energy on ballistic impact. The joint interface of two plates (plates #201P-03 and #201P-04) totally delaminated, and both display a low or no wave pattern on the as-bonded surfaces. The other plate, #201P-05, was only partially delaminated with two ballistic hits. The noticeable difference is that the wave pattern on this plate is much larger than the other two ballistically tested.

Several SEM photos were taken of the composite material in ballistically damaged areas. Photo 8 exhibits a brittle area of titanium at 500X magnification near the joint interface, and Photo 9 shows a classic ductile area of the titanium at 2500X magnification. Photo 10, at 5000X magnification, illustrates brittle transgranular failure of steel platelets, where numerous cracks are surrounded by a ductile matrix near the leading edge of the ballistically damaged region. Light microscopy of this ballistically damaged steel area shows that cracks are propagating downward toward the composite interface. Photo 11 exhibits a shear fracture at 50X magnification of steel.

Upon investigating the method used to produce these three armor plates, it appears that the timeliness of the surface cleaning of the titanium plates prior to explosive bonding may significantly effect the bond quality and ultrasonic test results. The three ballistically tested plates that passed 100% ultrasonic inspection were cleaned just hours before explosive bonding.

Ballistic Test Results from Phase II are shown in Table 2 and Photos 1 through 7. Table 2 identifies the projectile striking velocity and the measured V_{50} data. The photos show the location and extent of ballistic damage on the plate exterior. Note that the Phase I

ballistic tests caused the plates to debond after no more than two hits, while the Phase II ballistic testing indicates that the composite plates can withstand multiple hits.

Note also shows that the interior surfaces of the hi-hard surface have a ductile appearance rather than a conical shape. With the exceptions of plates 20 and 21, however, testing was stopped after plates delaminated. Although the progress from Phase I to II is significant, plate delamination could be further minimized by several methods discussed in other sections.

Explosive Bonding

Explosive bonding was conducted at New Mexico Tech-Energetic Materials Research & Testing Center in Socorro, N.M., under the guidance of Dr. Vasant Joshi. Testing involved a total of 25 explosive bonding shots. See Table 3 for a summary of this work and a list of the titanium/steel plate combinations. All titanium and Ti-6-4 plates measured 15" x 15". The titanium, grade 2 plates were purchased from Tico Titanium, Farmington Hills, Mich.; Ti-6-4 plates from Supra Alloys, Camarillo, Calif.; and Titanium Industries, Wood Dale, Ill.. The A2 and D2 tool steel plates were acquired from Alro Steel in Menomonee Falls, Wis., and the hi-hard plates were procured from Clifton Steel Co., Twinsburg, Ohio.

The objectives of the explosive bonding were as follows:

- Improve the as-bonded and as-heat treated joint strength by producing explosive bonded plates with a wavy interface.
- Investigate the use of an interlayer for explosive bonding (Ta, Mo, etc.).
- Develop a line wave generator system for 19" (15" plates + 4" momentum strips) and 34" (30" plates + 4" momentum strips) plates for all projected Phase II explosive bonding.
- Develop a momentum trap system that not only avoids or minimizes spall of the bonded steel plate but also breaks the shock caused by the line wave generator.
- Investigate emulsifiers for improved stability of the explosive wavefront.
- Investigate CO_2 jet cleaning for removing plate oxidation. (This process was unable to remove the surface metal oxide prior to bonding.)

One way to prevent or minimize the undesired intermetallics at the joint interface is to introduce a thin interlayer. Two candidates chosen were molybdenum and tantalum, each with a thickness of approximately .0005", based on the diffusion depth of the TiC intermetallic formation. The application methods studied to introduce the interlayer were electroplating, vapor deposition and spotwelded thin foils. Electroplating was found unsuitable for applying either metal.

Two of the first four explosively bonded plates had electron beam ion plated tantalum coatings. Plate #01 was ordered with a 150-angstrom thick coating but came with a 20,000-angstrom thick coating, which led to the plates failing to bond properly, most

likely due to the excessively thick film. However, Plate #04, which had a 150-angstrom thick tantalum ion plating, bonded 100%. Photo 12 is a SEM photo at 15,000X magnification showing the tantalum ion plated interface.

Another interlayer method chosen for further study consists of a composite plate with thin metal foils of tantalum, molybdenum, low carbon steel, and brass (Plate #03) spotwelded to the steel interfacial surface. These commercially available materials are limited in width and thickness - the thinnest tantalum and molybdenum being .0005", brass .001", and carbon steel .001" thick. These foil thicknesses were used, except for the carbon steel, which was .002" thick. Unfortunately none of these foils are commercially available in a 15" width. With only narrower widths available, usage would require foil overlapping or a gap between foils to cover a 15" x 15" plate size. Either condition could produce a localized weak bond during explosive bonding. Photo 13 depicts the brass interlayer at the interface.

Explosive bonding parameters were based on plates having a flatness of 1/16" or less and a thickness less than .260". Surface finish and cleanliness were also critical parameters. The explosive bonding setup is illustrated in Figure 1.

All plates were shipped to John Krebsbach, Adaptive Coating Technologies, Madison, Wis., for ultrasonic inspection and metallographic examination. The unbonded regions were identified and removed.

Methods for sectioning these plates at various stages were studied. The ideal candidate needed not only to be commercially available and cost effective but also cause no extreme heat during sectioning and no excessive corrosion of the steel. Waterjet, laser and bandsaw cutting, and EDM (electrical discharge machining) were investigated. Laser cutting was ruled out because thermal conductivity differences between the two materials are too wide and therefore unacceptable. Sawcutting was eliminated because it could section neither hardened steel nor a composite with any noticeable amount of hard intermetallic material. Also sawcutting would have produced waste material. Therefore waterjet and EDM were the preferred methods. EDM costs were projected at twice that of waterjet; however EDM did not have the corrosion or kerf concerns typical of waterjet cutting. In the end, waterjet was chosen, and precautions were taken to minimize potential kerf and corrosion concerns. Future work, however, should consider EDM, as the waterjet cutting costs for this project were much higher than projected.

Samples waterjet cut from longitudinal cross-sections of the composite bonded plates were examined using optical microscopy to study the explosive wave pattern. A number of points were chosen to ensure uniformity of the bond. After careful readjustment of the explosive bonding parameters, observations along the cross section were repeated, and four distinct wave patterns of bond interface were obtained, as shown in Photos 14-17. A smooth or waveless interface was targeted for minimizing the residual stresses. A fine, symmetric wavy interface was obtained in lower alloy plates. Fine asymmetrical and large asymmetrical waves were obtained in higher alloy plates.

Heat Treating

The heat treat work was conducted at Adaptive Coating Technologies, LLC, in Waunakee, Wis., under the guidance of John Krebsbach.

Objectives were as follows:

- Expand heat treat capability from tool steel to Hi-hard composite materials and from Ti to Ti-6-4 composite materials.
- Determine the minimum time-temperature parameters for proper stress relief, hardening and tempering to minimize interfacial diffusion.

In order to meet these objectives, a new IR furnace, controls and quench system was designed, fabricated and assembled. In addition, the furnace was changed from a vacuum furnace without quench capability to a positive pressure inert gas furnace with multiple quenchant capability.

To obtain the proper time-temperature parameters for stress relieving, hardening and tempering, the heat treating development process began with 1" x 1" steel composite specimens. A thermocouple wire was spotwelded at the interface through a hole bored into the center of the titanium portion of the specimen. To study the thermal gradient through the entire composite thickness, two more thermocouples were spotwelded on the steel and titanium surfaces for a total of three. After extensive testing, just two thermocouples were used to measure the steel and titanium surface temperatures.

The goal of hardening was to achieve a minimum hardness of 60 R_c for the tool steels and 45 R_c for the hi-hard through at least half the steel thickness. Because the hardening temperature for tool steel has to be above 1800°F and the titanium beta transus temperature is close to that, a thermal gradient was required between the steel and titanium to maintain the titanium interface below the beta transus. This thermal gradient was established by placing the titanium side of the composite plate onto a water cooled copper door. The beta transus temperature for titanium is 1745°F, and for Ti-6-4, 1830°F. Although similar or higher thermal gradients were achieved with the Phase II furnace compared to the Phase I, Phase II attempted to minimize the thermal gradient in order to lessen interfacial stress and excessive atomic diffusion while still maintaining the titanium temperature below the beta transus temperature. For the Hi-hard composites, no thermal gradient was required because the hardening temperature was 1590-1600°F for the steel portion.

To develop the time-temperature parameters for heat treating the various steel material types, extensive hardening and tempering tests were done using .25" thick metallographic and U-bend specimens of each material type. This information was another ingredient used to develop the final heat treat parameters for the composite test specimens and ultimately the ballistically tested plates. In Phase I, the tool steels were heated to 950°C (1742°F) for a minimum of 20 minutes, per standard commercial practices. Unlike Phase I, Phase II focused on the minimum time to achieve the maximum steel hardness; thereby

minimizing atomic diffusion at the composite interface. To achieve maximum hardness, the optimum time for heating tool steel composites is 10 minutes or 600 seconds at 1850°F, while the optimum time for Hi-hard is 60-70 seconds at 1590-1600°F.

To minimize thermal stress, reduce plate bow and improve temperature uniformity, the final six Hi-hard composite plates were placed inside the furnace titanium side up, which is the concave side up. Upon heating, the titanium surface temperature was higher than that of the steel surface but below the beta transus temperature. Thus the thermal stresses at the joint interface were minimized, as the thermal expansion of Hi-hard steel is higher than that of titanium. Heating the plates titanium side up also reduced the bow, which is necessary because the composite plates cannot be straightened satisfactorily with a straightening press after heat treating without cracking. In addition, the uniformity of the steel temperature was improved by placing the titanium side up because the plate was heated by conduction rather than direct radiation.

To quench the tool steels after the proper austenitizing time-temperature parameters were met, inert gas flow was used to cool the steel surface temperature below the critical pearlite nose of the time-temperature-transformation curve. For A2, quenching parameters require that the material temperature drop from the austenitizing temperature to 1300°F in six minutes, and for D2, to 1300°F in four minutes. Hi-hard steel quenching parameters require that the material temperature drops from the austenitizing temperature to 900°F in approximately 10 seconds. Suitable quenchants - including polymer, oil, water baths and spray quenching - were investigated for producing hardened Hi-hard composite plates. Oil and polymer quenching resulted in significantly lower surface hardness than water quenching. In the end, water quenching in an agitated tank was the chosen method.

In addition, spray quenching, which uses high pressure nozzles and a water or polymer quenchant to cool a part rapidly enough to attain good hardness, may be a worthwhile alternative. Spray quenching is a directional process that can cool the low thermal expansion titanium last, thereby minimizing joint interfacial stress. On the other hand, spray quenching of large plates may raise stress levels, due to possible non-uniform cooling rates. Another concern is that the quenching process may not cool the steel plates quickly enough to develop the desired plate hardness. Because the quantity of composite plates available was much less than that required to develop suitable spray quenching parameters, this work could not be pursued at this time.

After quenching, the hardened composites were tempered at various temperatures, 350°F for an hour for the Hi-hard composites and double tempered at 400°F for one hour for the tool steel composites.

The graphs in Figures 6.1 through 8.2 represent the hardness and bend test data for Hi-hard and A2 steel composite materials. Figure 6.1 and 6.2 are compilations of data showing the relationships between hardness and bend angle at various soak temperatures and constant soak times. Likewise, Figures 7.1 and 7.2 are collections of hardness and bend angle data at various soak times and constant soak temperatures. Lastly, Figures 8.1

and 8.2 show miscellaneous information. All this data helped determine the hardening parameters for the Hi-hard plates submitted for ballistic testing.

The tantalum interfacial thicknesses specified for plate numbers 01 and 04 are based on the diffusion of titanium and carbon at the anticipated time-temperature hardening parameters for A2 tool steel/titanium.[24]

Although Phase II proposed using M2 tool steel, it became apparent after experimentation with the infrared furnace, that the 2175-2250°F austenitizing temperature would be extremely difficult to attain and would damage all high temperature sealing surfaces very rapidly.

Other limited testing performed for possible economic or ballistic improvements included TLP melting , depositing and fusing hard coatings to the steel surface, and dissimilar metal brazing. Transient Liquid Phase (TLP) melting was investigated as a possible alternative to explosive bonding to minimize the cost of producing a composite material. TLP, a thermal process that usually consists of applying a very thin interlayer foil between two dissimilar materials, was not attempted due to intermetallic formation and elimination issues.

Two tests were conducted to determine whether a hi-hard material could have brazing tapes applied to the surface and metallurgically bonded to improve the surface hardness of the Hi-hard material. The first test concluded that tapes could be applied and fused on a hi-hard steel specimen to provide a 60 R_c+ hardness while enabling a 180° bend angle without any visible signs of delamination or cracking of the coating. The second test successfully bonded and fused the coating, as well as heat treated the hi-hard substrate. Again the specimen was able to withstand a 180° bend angle without any visible signs of delamination or cracking of the coating.

Brazing of individual tool steel and titanium plates was also investigated using copper and Gapasil foils manufactured by Wesgo. But during heating, the steel decarburized and prevented either foil from wetting the surface. Likewise, during heating, the titanium oxidized enough to prevent wetting of either foil material. Copper plating of the steel and titanium surfaces allowed the copper foil to wet both surfaces well, but caused erosion of the titanium. As expected, the Ti-Cu interface exhibited extensive amounts of intermetallic formation at the joint interface. Vacuum furnace brazing of this material composition, however, may be a more suitable option. Note that a brazing study was conducted early in the project. Significant improvements were made that drastically reduced furnace oxygen levels, but the brazing test was not rerun.

After plates 20 through 25 were explosively bonded and ultrasonically inspected, they were grit blasted with a spherical zirconia bead to remove surface oxidation prior to heat treating. In order to remove the stress due to explosive bonding in both the composite materials, the plates were stress relieved at 1050°F for four hours prior to hardening.

In July and August, 1999, these same six 12" x 12" plates were heat treated in a 15" x 16" infrared furnace at 1600°F for 60-70 seconds, then water quenched in an agitated tank. The hardened composite plates were tempered for one hour at 350° and forwarded to ARL/ Mr. Matt Burkins for ballistic testing.

Inspection

1. Metallographic Test Results

Before metallographic examination, the 1" x 1" inch thick as-received, as-bonded and as-heat treated specimens were sectioned, mounted and polished. Each photomicrograph represents the respective material condition and location.

The as-received Hi-hard material, in Photo 18 #1131 at 500X magnification, exhibits a banded arrangement of ferrite and pearlite. The hardened Hi-hard material shows a martensitic structure in Photo 19 #1136 at 500X magnification, and the hardened and tempered Hi-hard in Photo 20 #1134 at 500X magnification presents a tempered martenistic structure. The as-received Ti-6-4 material in Photo 21 #1139 illustrates a lamellar titanium structure.

When the steel and titanium materials were explosively bonded, the as-bonded Hi-hard/Ti-6-4 components retained the same microstructures in the composite as they do in the bulk state, as previously shown. However, the interface is similar to the other heat treated composites that exhibit cracks at the crest of the wave in the brittle intermetallic region. Similar features are noted in the hardened Hi-hard/Ti-6-4 illustrated in Photo 22 #1126 and the hardened and tempered Hi-hard/Ti-6 in Photo 23 #1137, both at a magnification of 200X. The steel material specimens were etched with a 2% nital solution, and the titanium specimens were etched with a Kroll's reagent.

It's important to note that no brittle region or cracks are visible at the interface of any of the A2/Ti composite specimens with the 150 angstrom thick layer of tantalum, as shown in Photo 24 #1086.

2. Microhardness Data

Microhardness data was gathered on specimens at critical processing stages. Typical results are shown in Figure 2 and Tables 4 and 5. Multiple hardness readings were taken at the various metal surfaces to investigate oxidation and decarburization changes. In addition, the interfacial regions were studied to investigate the presence of intermetallics. The presence of any of these features would increase the hardness at the respective surfaces. The only sharp increase appears with the as-bonded composite at the steel surface.

Also, tempering heat treatment seems to have no significant effect on the hardness of the steel or titanium constituents.

3. Ultrasonic Testing

All as-bonded plates were 100% ultrasonically inspected from the steel surface. Results are presented in Table 3, which shows that typically the explosive bond appears to be weaker or more highly stressed in the two areas that are parallel to the explosive wavefront and at each end of the composite plate. These entrance and exit regions are also the most highly bowed from the center, with the exit end displaying some spalling of the steel constituent.

4. U-Bend Test Results

A series of three point bend tests using a hydraulic press retrofitted with a 1.50" diameter mandrel with a crosshead travel speed of approximately .12 in/sec was conducted on .25" wide x 6" long specimens. Testing looked at the ductility of the starting materials and the ductility after the major processing steps, as listed in Figures 6.1 through 8.2. Note that the graphs have two sets of data points. The first set, denoted by the darker symbols and the corresponding darker line, shows the hardness data. The second set, designated by the same symbol shapes and lines only lighter, shows the bend data. The specific failure mode is detailed in Table 6.

Bend testing was the main criteria for determining the optimum stress relief time-temperature parameters. For example, initial tests at a stress relief of 350°F for 1 hour resulted in a 37° bend angle, while a stress relief at 1050°F for four hours produced a bend angle of 89°. No bend testing was performed on the composite plate with the tantalum interlayer, due to insufficient plate size.

5. XRD Test Results

Several A2/Ti as-bonded specimens were removed from Phase I plate #201P-09 for X-ray diffraction testing. The unit used was a Phillips X-ray diffraction system 1080 and utilized specimens less than 1 cm^2.

6. Ballistic Simulation Modeling

EMRTC simulated the damage of various composite plates from the impact of a standard bullet (M2AP). To determine the effect of material variables on bullet damage and penetration, computer simulations were done for different impact velocities - 2500, 2700, 2800 and 3000 feet per second. Testing was based on unconfined cylindrical composite pieces 2-4" in diameter and .450" thick. The thickness of the composite was identical to the actual plates. This code was developed at New Mexico Tech and has shown good correlation between experiment and simulation of a bomb case disintegration. For the first simulation test, the bullet was S7 tool steel; all other tests considered it a 1090 steel hardened to 63 R_c. A set of images showing material, position, pressure and velocity plots of the various simulations is shown in videotape format and condensed in Table 7.

Note that the simulations were performed without consideration of damage accumulation. At 2500 fps, a M2AP bullet impacting a .250" steel/.225" titanium composite should stop in the titanium layer. At 2700 fps, the bullet should produce full penetration, unless a hard surface layer of sufficient hardness, such as a 1-2 mm thick layer of TiB_2, is on the steel surface. Likewise, the same relationship is representative of 2800 and 3000 fps bullet velocities.

7. Impact Test Results

Figure 3 illustrates the Dynatup test results of five A2/Ti as-bonded specimens. Impact testing was performed in accordance with ASTM E-23. A 20,000# tup capacity was used with a full pendulum drop at 17.5 fps. The x-axis represents time in milliseconds, and the left y-axis represents load corresponding to the load line. The leftmost line and the right y-axis represents the energy absorbed by the specimen. From time t=0 to point "+" the steel and titanium material are in an elastic condition. From "+" to "1", the steel is yielding with 6.40-28.12 ft-lb energy absorbed; "3" represents the loss of bond or possibly the titanium yield point, and "5" is the complete specimen failure. See the data in Table 8.

8. Residual Stress Data

Two 1" x 1" x .5" A2/Ti as-bonded composite specimens #9 and #10 removed from Phase I plate #201P-09 were tested to determine longitudinal subsurface residual stress distributions. Results are shown in Tables 9 and 10 and graphed in Figures 4 and 5. X-ray diffraction residual stress measurements were made from the surface to nominal depths of 250×10^{-3} inches at eight different depths. Measurements were made in the longitudinal direction on the steel side for Sample #10 and on the titanium side for Sample #9. For subsurface measurement, material was removed electrolytically to minimize the possible alteration of the subsurface residual stress distribution due to material removal.

The residual stress data for the titanium side of the composite specimen is stated in Figure 4. The results show near surface tension as high as +12 ksi. The distribution shows that the maximum compression is about –15 ksi and that the residual stress returns to tension in the final depths of the profile. The (21.3) peak width results for the titanium indicates an increase in hardness or cold working as depth is increased.

The residual stress results for the steel side are shown in Figure 5. The data indicates surface tension on the order of +60 ksi. The distribution crosses into compression and reaches a maximum compression of about –5ksi. The (211) peak width data shows a decrease in hardness or cold working as a function of depth.

9. Other

Plate bow from Phase I varies from .050" to .250", depending on plate and measurement direction. Plate bow from Phase II plates varies from .131" to .404", which is mostly attributable to the higher energy levels required to create the wavy interface. Removing

or eliminating this condition has proved difficult. (See the Conclusions and Technical Substantiations section.)

Lap shear and tensile testing were also conducted. Three lap shear specimens, #28-30, were removed from the Phase I as-bonded A2/Ti composite plate #201P-09. Two tensile test specimens were removed from plate #04. Results indicate 15,100 psi and 16,600 psi tensile strength from the Ta specimens, and 10,276 psi lap shear strength for plate #03 specimens.

C. Conclusions and Technical Substantiations

1. Fabricated an alternate armor by explosive bonding several dissimilar steel and titanium materials with widely varying physical and mechanical properties to form unique composites that could be used as armor.

2. Investigated interlayer materials between the steel and titanium components. A tantalum interlayer applied prior to explosive bonding Hi-hard steel and Ti-6-4 appears to improve ballistic performance without producing significant levels of intermetallic formation or cracking at the interfacial region. Until recently, no method for applying a uniform coating thickness over an 8" diameter plate had been found. However a supplier has been located to apply thin films on 15" x 15" plates, or perhaps larger, which may allow for a straightening press to remove plate bow after explosive bonding. But optimization of the interfacial thickness is still needed to ensure adequate separation of materials and maximize joint ductility and bond strength.

3. It is possible to explosively bond Hi-hard and Ti-6-4 with a wavy interface that does not delaminate during heat treating. This new lightweight composite armor has also been shown to endure multiple ballistic hits before plate failure, unlike Phase I. Recent ballistic testing at US Army Research Laboratory in Aberdeen, MD, demonstrated that ½" thick steel/titanium composite plates have V50 data 25% higher than V50 data for Equal Area Density of RHA (MIL-A-12560) using M2AP projectiles. The V50 data for the new material is in excess of 800 m/sec. The V_{50} for equal area density of RHA(MIL-A-12560) is 658 m/sec. This armor is approximately 22% lighter than ½" thick hi-hard armor.

4. Determined the likely cause of the delamination failures during ballistic testing of the Phase I plates.

5. Finding a method of eliminating plate bow after explosive bonding is critical. To remove the bow using a straightening press without an interlayer resulted in interfacial cracking, probably due to the presence of brittle intermetallic materials. The three ways found to reduce plate bow are: (a) establish a thermal gradient within the material thickness when heat treating the composite in the IR furnace, (b) increase the width of the side momentum strips from 2" to 5", and (c) have the explosive

wavefront proceed an additional 5" off the end of the composite plate. Widening the ANFO beyond the plate at least 4-5 inches on the exit end and on both sides would reduce the bow approximately 30%.

6. Ballistic modeling identifies that at 2500 fps, a M2AP bullet, impacting a .250" steel/.225" titanium composite, should stop in the titanium layer. At 2700 fps, the bullet should produce full penetration of the same composite, unless a hard surface layer of sufficient hardness, such as a 1-2 mm thick layer of TiB_2, is on the steel surface. Likewise, the same relationship is representative of 2800 and 3000 fps bullet velocities for steel/Ti-6-4 composite plates.

7. Surface quality of the plates prior to explosive bonding - including roughness, flatness and cleanliness - is critical to adequate adhesion between flyer and backer plates.

8. It is possible to metallurgically fuse a hard 60 R_c coating onto Hi-hard whereby the steel substrate is simultaneously hardened. Such a coating-substrate combination can withstand a 180° bending without delamination or cracking of the coating.

9. Infrared heating can harden Hi-hard and tool steels quicker than commercially accepted time parameters to minimize atomic diffusion and aid in reducing the plate bow caused by explosive bonding.

10. With infrared heating, a post heat treatment can attain a minimum of Rockwell C45 microhardness throughout more than half of the Hi-hard steel thickness without causing a significant deleterious effect on the titanium. Hardnesses of the Hi-hard steel climbed from an average 22 R_c to 46 R_c as a result of infrared heating. Likewise, the titanium stayed the same, 33 R_c, during the same cycle.

11. Plate material types were expanded to include an almost unlimited variety of materials, due to the expanded flexibility of the heat treating portion of this work. Previously in Phase I all proposed composite materials were limited to air hardening tool steels; however because of process changes, carbon, alloy and most tool steels became eligible for the steel component.

II. Detailed Description of Analytical Methods/Results

A. Explosive Bonding

The chemistry of the as-received plates is shown in Table 11. The titanium was certified to meet the requirements of ASTM B-265 and ASME SB-265, grade 2. Ti-6-4 met a variety of specifications, including ASTM B-265-95 and MIL-T-9046 minimum. The

Hi-hard met MIL-A-46100. Mechanical properties for the various materials are shown in Table 12.
Prior to explosive bonding, the final Hi-hard steel and Ti-6-4 plates were inspected and shipped to New MexicoTech in Socorro, N.M. The Hi-hard plates were purchased in the annealed condition and surface ground on both sides, while the titanium plates were left in the as-received condition. All original plates were 15" x 15".

In all cases, the explosive bonding used a titanium flyer plate and a hi-hard steel backer plate. A .2" standoff between the plates was maintained by a foam or steel tube. See Figure 1. The tool steel plates had 2" wide momentum strips tack welded around the entire plate. A cardboard barrier was glued to the titanium flyer plate to retain the explosive, and the two plates and cardboard barrier were then duct taped together.

At the explosion site, the taped assembly was placed on a 1" thick steel anvil plate on top of a mound of compacted sand. A Dupont Detasheet C4 strip was placed along the 19" plate width (15" plate plus 4" momentum strip widths), and the cardboard barrier was filled with ammonium nitrate fuel oil prills up to a height of 3.0". This prill volume was calculated to yield a 3.2-3.5 km/sec detonation velocity. An ordnance person then placed the two detonators in the center of the Detasheet, and ignited the charge with an RP 83 detonator.

The explosive bonding parameters, including flyer plate velocity and position at impact, were developed using the MY1DL program. This program is a one dimensional Lagrangian hydrocode based on the difference equations by Neumann and Richtmyer[1]. The MY1DL program can calculate time-distance-pressure and position during shock loading, as well as energy input during passage of the shock wave. Shock waves are treated as a mathematical discontinuity across which Rankine-Hugoniot relations are applied; and the concept of artificial viscosity makes it possible to calculate the steep increase in the pressures near the shock front. The various materials for flyer plate, impacted and compressed materials are discretized by cells, so that the basic equations can be substituted by finite difference elements. As the cell size becomes smaller, the finite differences approach the actual differences.

Lagrangian hydrocodes are generally simpler than Eularian hydrocodes, as they involve constitutive models. The MY1DL program uses the Mie-Gruneisen equation of state for the extension of the shock Hugoniot (experimental) and the thermal expansion at ambient pressure, into the adjacent regions in energy-pressure-volume (e-p-v) Equation of State (EOS) space. For the explosive bonding, Gamma law approximations were used.

The input requires material densities, shock Hugoniot coefficients (C and S), specific heats and thermal expansion coefficients. The output for various cells gives pressure, temperature, energy and particle velocities. The program requires extensive knowledge of shock-wave theory and is reasonably accurate for estimation of pressure-time (p-t), particle velocity-time (u-t), and velocity-time (v-t) profiles.

The use of an interlayer material appears to be a suitable alternative for creating a stronger bond joint. Electroplating methods, including surface metallizing, indicated that

neither molybdenum nor tantalum films could adhere to the steel or titanium surfaces. Vapor deposition methods seemed to show more promise with the coating-substrate combinations. However, most commercial vapor deposition vendors could only apply these coatings on substrates eight inches in diameter or smaller, and the vendors capable of applying a coating on 15" x 15" plates would not bid on the work because of the low part volumes. For the deposition equipment designed for 8" diameters, it's estimated that coating thickness on larger substrates decreases approximately 10% per inch outside that 8" diameter, and the decrease in adhesion is unknown.

Variation in the plate condition prior to bonding, including surface cleanliness, flatness, thickness and parallelism, is a critical parameter. In addition, inclusion of metal foils as an interlayer in a composite plate must take into account the foil thickness, width and methods of attachment. Thin metal films deposited onto substrate surfaces must consider coating thickness, coverage areas and uniformity issues.

Figures 10 and 11 show the calculated flyer plate velocity and the titanium impact face position at various times with the ammonium nitrate/fuel oil mixture used in this work.

B. Heat Treating

Initial hardening and tempering parameters were based on time-temperature transformation data for the various steel materials. The final heat treating parameters for the six ballistically tested plates were primarily based on the hardness and bend test data accumulated during this project.

Initially 1" x 1" specimens were machined to locate insulated K type thermocouples. These thermocouples were used to measure the joint interface temperature as well as the titanium and steel surface temperatures. Due to the machining required to locate and attach these thermocouples, this methodology consumed a lot of time and provided limited thermal gradient information, which was primarily used for the tool steel composite materials. Later testing had thermocouples spotwelded to each face of the composite specimen only. This method was less time consuming and yielded good temperature readings. When tool steel composites were heat treated, a copper or stainless steel powder was placed between the composite plate and water cooled copper plate to compensate for any distortion in the specimen caused by explosive bonding or heat treating.

The IR furnace consisted of a custom designed gold plated 15" x 16" chamber with a copper cooled hinged door. The furnace had multiple gas entry ports. A positive pressure was applied using a 99.999% high purity argon to purge the chamber. Multiple gas exit ports were piped to a vacuum pump, which operated before and during the hardening process to reduce the oxygen levels in the furnace to acceptable levels. The exit gas was monitored by an Advanced Instruments GPR-16 oxygen analyzer and recorded. When the oxygen level in the furnace was as low as possible, but never above 10 ppm, heating was started. Chamber pressure was maintained at a positive 5-10" WC.

The furnace was close-loop controlled on one of the K-type thermocouple wires. Two thermocouples were attached to show the widest variation in temperature, which is attributable to the plate out-of-flatness condition. On the final plates submitted for ballistic testing, one thermocouple was in the middle of the plate on the steel surface; the other on the outside edge of the steel. A tweezer spotwelder was used to attach thermocouples to both the titanium and steel material surfaces.

Early in the heat treating development phase, the oxygen levels were higher than desired. This situation was managed by establishing good sealing surfaces prior to heating and preventing seal degradation during the heating process.

The actual time-temperature data was recorded during infrared heating, and a chart showing the thermal gradient between the titanium and steel materials is shown in Figure 9. The x-axis measures time and the y-axis measures temperature in Fahrenheit with the maximum value representing 2000°F. The highest temperature recorded is at 1800°F representing the steel surface temperature. The interface is at 1640°F, and the titanium surface temperature is at 1200°F, for a total thermal gradient of 600°F. The chart recorder was a Yokogawa 3 pen unit that simultaneously recorded oxygen levels and two temperature readings. In order to reach the required hardening temperature and minimize the thermal shock between the two materials, those plates submitted for ballistic testing required longer ramp times than the test specimens.

When hardening the tool steel composite specimens at the proper austenitizing temperature for the proper length of time, the furnace was de-energized and the part was quenched. The heat flow through the composite was controlled by the water cooled copper door removing the heat through the titanium side. Likewise the inert gas flowing through the furnace was used to cool the steel surface, leaving the interfacial region to cool last.

When hardening the Hi-hard composite specimens and after the proper austenitizing temperature/time was reached, the specimens were quenched in a tank filled with water. The water was thoroughly agitated using air or electric motors.

To avoid pearlite formation, quenching needed to reduce the specimen temperature to 1300°F (704°C) from the austenitizing temperature in less than six minutes for A2 and less than four minutes for D2 tool steels. The Hi-hard steels had to be quenched in seconds; thereby requiring water, oil or polymer quenching for adequate hardness. No specimens were subjected to cryogenic cooling to achieve a higher martensitic percentage and the corresponding higher tool steel hardness values. Table 13 illustrates the thermal history for the plates submitted for ballistic testing.

Tempering of all test specimens and plates was done in the infrared furnace. During the tempering cycle, no thermal gradient was required through the composite thickness, regardless of the composite material types. To maintain a high A2 or D2 tool steel

hardness, the maximum tempering parameters were determined to be 205°C (400°F) for one hour. The Hi-hard steel was tempered at 350°F for one hour.

Infrared energy is the portion of the electromagnetic spectrum between .78 and 1000 microns. The actual emission of a given source is dependent upon its temperature. Increasing the source temperature results in shorter overall wavelengths. The emissive energy is related to the following equation:

$Q=KT^4$

Q-Total Emissive Power (watts/cm^2)
K-Stefan Boltzmann Constant=5.56×10^{-12}
T-Absolute Temperature (K)

Parameters of importance with high density infrared heating are defined in the following equation:

$Q=(FV) \times (ES) \times (AT) \times (K) \times (TS^4 - TT^4)$

Q-Heat transfer between the source and target (watts/cm^2)
FV-View factor between the source and target
ES-Emissivity factor of the source
AT-Absorption factor of the target
K-Stefan Boltzmann Constant
TS-Absolute Temperature of the source
TT-Absolute Temperature of the target

The view factor term is the fraction between 0 and 1 that quantifies the amount of radiant energy emitted from the source that falls incident upon the target. The absorbed heat transfer (Q) results in a temperature rise of the target as defined by the following equation:

$T=(Q) \times (A) \times (t)/(M)/(C_p)$

T-Product Temperature Rise (°C)
A-Area of target (cm^2)
t-Heating dwell time
M-Mass of the target
C_p-Target specific heat (Watt-sec/kg -° C)

C. Inspection

Metallographic Test Results

The metallographic specimens were sectioned from the corresponding heat treated plates using a Leco VC-50 low speed diamond saw. The specimens were then cold mounted in epoxy, and the

cured specimens were ground and polished using a Struers DAP-V/Pedemin unit. Photomicrographs were taken with a Versamet microscope and 4" x 5" Polaroid 54 film.

Microhardness Data

Microhardness testing was performed with a Shimadzu Type M microhardness tester using either a 100 gm or 300 gm load for 30 seconds.

Ultrasonic Testing

Ultrasonic inspection of the 15" x 15" plates was conducted using an NDT Systems Inc., Nova Eclipse TG-2 handheld ultrasonic detector and a C11, .125" diameter, 5 MHz transducer with a 0 degree impingement angle. Commercial grade glycerine was used as the couplant. Plates were protected to prevent the couplant from penetrating into the bond joint.

U-bend Test Results

Numerous bend tests were conducted first using the individual steel or titanium materials in the as-received, hardened, and hardened and tempered states. These values were used as a baseline prior to testing the various composite specimen material combinations and heat treating conditions. The results are presented in a condensed form in Table 6. Notice that regardless of the heat treat parameters used for the individual Hi-hard and the A2 tool steel specimens, the bend test results are usually 180°. The individual D2 specimens have low bend values compared to the other steels irregardless of heat treating parameters.

The failure mode for the .25" x 6" long composite specimens was either delamination or fracture. Specimens failing by delamination initially started delaminating from one end, and this feature was not always visibly or audibly apparent. As bending continued, delamination progressed along the specimen length until the entire composite specimen had separated or debonded, and it was apparent during testing when the composite specimens totally delaminated. As a result, the delamination values in the table reflect this effect.

Some of the composite specimens fractured in the titanium rather than delaminated. This fracture occurred in the highly stressed regions directly below the mandrel radius, which may indicate a strong interfacial bond or the possibility of exceeding the beta transus temperature during the hardening process.

These bend test delamination failures are believed to correlate to the extent of brittle intermetallic formation present at the interface. The elimination of these intermetallics through the use of an interlayer are believed to greatly improve the bending strength of the various composite plates.

Also when bend testing was performed on plates significantly thicker than .250" - such as plates #14, 16 and 17 - the specimen delaminated earlier than expected due to the weaker bond formed during explosive bonding.

XRD Test Results - Further Details

XRD examination of a ballistically tested plate shows TiC, FeO, FeV, FeTi, Cr_2Ti, Cr_7C_3 and $Cr_{.36}Fe_{.52}$ intermetallic formations in the interfacial region. Because a TiC formation is mainly exothermic and a volume change is associated with this reaction, weakening at the interface on an atomic level is probably occurring. Whether or not formation occurs during bonding or heat treating, the minimization or elimination of TiC is strongly desired.

Ballistic Simulation Modeling

A three-dimensional (axi-symmetry) Smooth Particle Hydrodynamic code MAGI developed at New Mexico Tech was used. This program has shown good correlation between the experiment and simulation of a bomb case disintegration.

Residual Stress Data

X-ray diffraction residual stress measurements were made from the surface to nominal depths of 250×10^{-3}" in approximately eight depths. For subsurface measurement, material was removed electrolytically to minimize possible alteration of the subsurface residual stress distribution. All data obtained as a function of depth was corrected for the effects of the penetration of the radiation for the residual stress measurement into the subsurface stress gradient.[32] The stress gradient correction applied to the last depth measured is based on an extrapolation to greater depths and may result in over correction at the last depth, if the stress profile has been terminated in the presence of a steep gradient. Corrections for sectioning stress relaxation and for stress relaxation caused by layer removal[33] are applied as appropriate.

The longitudinal residual stress distributions measured as functions of depth are presented in Tables 9 and 10 and are shown graphically in Figures 4 and 5. Compressive stresses are shown as negative values; tensile as positive, both in units of ksi (10^3 psi) and MPa (10^6 N/m^2)

X-ray diffraction residual stress measurements were performed using a two-angle sine-squared psi technique, in accordance with SAE J784a. Diffraction of chromium and copper K-alpha radiation from the (211) and (21.3) planes of the BCC and HCP structure of the steel and titanium, respectively, were employed. The diffraction peak angular positions at each of the psi tilts were determined from the position of the K-alpha 1 diffraction peak separated from the superimposed K-alpha doublet, assuming a Pearson VII function diffraction peak profile in the high back-reflection region.[30] The diffracted intensity, peak breadth and position of the K-alpha 1 diffraction peak were determined by fitting the Pearson VII function peak profile by least squares regression after correction

for the Lorentz polarization and absorption effects and for a linearly sloping background intensity.

Details of the diffractometer fixturing are outlined below:

Incident Beam Divergence:	1.0 deg.
Detector:	Si(Li) set for 90% acceptance of the chromium and copper K-alpha energy
Psi Rotation:	10 to 50 deg.
Irradiated Area:	0.2 x 0.4 in. (short axis in the direction of measurement)

The value of the x-ray elastic constant, $E/(1 + v)$, is required to calculate the macroscopic residual stress from the strain measured at a right angle to the (211) and (21.3) planes of 1050 steel and titanium. This stress-strain information was previously determined empirically([31]) by employing a simple rectangular beam of steel and titanium loaded in four-point bending on the diffractometer to known stress levels and measuring the resulting change in the spacing of the (211) planes in accordance with ASTM E1426-91. No attempt was made to determine the x-ray elastic constant of the steel in the composite specimen.

The results in Tables 9 and 10 for macroscopic residual stress data are given first as measured, then as corrected for the penetration of the radiation in the subsurface stress gradient, and finally for stress relaxation, which results from material removal by electropolishing of material layers for subsurface measurement and sectioning. The fully corrected data, shown in the column titled, "Relaxation," is plotted in the associated figure. The angular width of the (211) K-alpha 1 diffraction peak at half height is shown in the far right-hand column.

In each Figure 4 and 5, the macroscopic residual stress distribution is plotted in the upper graph. The lower graph gives the (211) diffraction peak width distribution, which was calculated simultaneously with the macroscopic residual stress. The (211) diffraction peak width is a sensitive function of the chemistry, hardness and degree to which the material has been cold worked. In martensitic steels, plastic deformation, commonly produced by processes such as shot peening or grinding, will cause work softening and a reduction in the peak width. In work hardening materials, the diffraction peak width increases significantly due to an increase in the average microstrain and a reduction of crystallite size produced by cold working. The (211) diffraction peak width can be indicative of how the material may have been processed and the depth to which it has been plastically deformed.

The error for each residual stress measurement is one standard deviation, resulting from random error in the determination of the diffraction peak angular positions and in the empirically determined value of $E/(1 + v)$ in the <211> direction. An additional semi-systematic error on the order of $\pm$ 2 ksi ($\pm$ 14 MPa) may result from sample positioning and instrument alignment errors. The magnitude of this systematic error was monitored

during the course of this investigation using a powdered metal zero-stress standard in accordance with ASTM E915 and was found to be +0.8 ksi.

Other

A portable two color infrared thermometer was tested to determine whether or not it could monitor the part surface temperatures during heat treating. However, the unit, chosen for its insensitivity to emissivity variations, measured the source temperature instead of the part surface temperature and was discontinued.

Conclusion

In conclusion, this work demonstrates significant benefits to explosively bonding two materials coupled with infrared heating. This overall process may hold great promise for producing a steel/titanium composite armor plate.

III. References

1. J. Von Neumann and R.D. Richtmyer, "A method for the numerical calculation of hydrodynamic shocks", Journal of Applied Physics, 21, 1950, pp 232-237.
2. M. Yoshida, "Program MY1DL-One Dimensional Lagrangian Hydrodynamic Code", New Mexico Tech, Socorro, NM, 1986, pp 1-48. 1. ASM Committee on Explosive Welding.
3. ASM Metals Handbook, Ninth Edition, Volume 6, "Explosive Welding", Welding, Brazing and Soldering, 1983.
4. Barbour, Richard T., "Pyrotechnics in Industry", McGraw-Hill, 1981.
5. "Materials Properties Handbook: Titanium Alloys", 1994.
6. ASM Metals Handbook, Volume 4, Heat Treating, 1991
7. Blue, C.A., Blue, R.A., Lin, R.Y., Lei, J-F, Williams, W.D., "Infrared Joining of Titanium Matrix Composites, Proceedings of the American Society for Composites, 1994.
8. Carpenter, S.H., Wittman, R.H., Annual Review of Materials Science, ed. Robert A. Huggins, Explosive Welding, Annual Reviews, Inc., Palo Alto, CA, p.177-199, 1975.
9. Hardwick, R., Explosive Welding for Metal Joining, p. 586-589.
10. Blazynski, T.Z., Dynamically Consolidated Composites: Manufacture and Properties,
11. Zimmerly, C.A., Inal, O.T., Richman, R.H., Explosive Welding of a Near-Equiatomic Nickel-Titanium Alloy to Low-Carbon Steel, Materials Science and Engineering, A188, p251-254, 1994.

12. Inal, O.T., Szecket, A., Vigueras, D.J., Pak, H-r, Explosive Welding of Ti-6Al-4V to Mild Steel Substrates, J. Vac. Sci. Technol. A, Vol. 3, # 6, Nov/Dec. 1985.
13. Jaramillo, D., Szecket, A., Inal, O.T., On the Transition from a Waveless to a Wavy Interface in Explosive Welding, Materials Science and Engineering, p. 217-222, 1987.
14. ASM Specialty Handbook: Tool Materials, 1995.
15. Vander Voort, G.F., Atlas of Time-Temperature Diagrams for Irons and Steels, ASM Intl, 1991.
16. Touloukian, Y.S., Kirby, R.K., Taylor, R.E., Desai, P.D., Thermal Expansion: Metallic Elements and Alloys, Volume 12, 1975.
17. Chandler, H., Heat Treater's Guide: Practices and Procedures for Iron and Steels, 2nd Edition, ASM Intl, 1995.
18. Latrobe Steel Company A-2 Tool Steel Data Sheet, 4/1992.
19. Kleven, S., "Ultrasonic Inspection of Explosion Welded Titanium Clad Plate", Materials Evaluation, May 1996, pp.557-560.
20. Touloukian, Y.S.,Thermophysical Properties of Matter, Volume 1, Thermal Conductivity-Metallic Elements and Alloys, ISI/Plenum Publishing, NY1970.
21. Touloukian, Y.S.,Thermophysical Properties of Matter, Volume 1, Thermal Conductivity-Metallic Elements and Alloys, ISI/Plenum Publishing, NY1970.
22. ASM International, "Heat Treater's Guide:Practices and Procedures for Irons and Steels, 2nd edition, 1995.
23. Gooch, W.A., Burkins, M.S., Ernst, H.-J., Wolf, T., "Ballistic Penetration of Titanium Alloy Ti-6Al-4V", Lightweight Armour Systems Symposiom '95, June 28-30, 1995.
24. Sarian, S., "Diffusion of Carbon in Titanium", Journal of Applied Physics, Vol. 39, Number 7, June 1968.
25. P.S. Prevey, *Adv. in X-Ray Anal.,* Vol. 29, 1986, pp. 103-11 1.
26. P.S. Prevey, *Adv. in X-Ray Anal.,* Vol. 20, 1977, pp. 345-354.
27. D.P. Koistinen and R.E. Marburger, *Trans. ASM,* Vol. 51, 1959, pp. 537-550.
28. M.G. Moore and W. P. Evans, *Trans. SAE,* Vol. 66, 1958, pp. 340-345.
29. Joshi, V., Banks, M., Krebsbach, J., Paper presented and accepted for publication in Shock Compression of Condensed Matter APS, A& P Press, June 27-July 2,1999,
30. Prevey, P. S., Adv. in X-ray Anal., Vol. 29, 1986, pp. 103-111.
31. Prevey, P. S., Adv. in X-ray Anal., Vol. 20, 1977, pp. 345-354.
32. Koistinen, D. P., and Marburger, R. E., Trans. ASM, Vol. 51, 1959, pp. 537-550.
33. Moore, M. G., and Evans, W. P., Trans. SAE, Vol. 66, 1958, pp 340-345.

Table 1. Phase I Ballistic Test Results

Shot		Cart Data (Wts Grns)		Velocity		Yaw	Penetration Description and Comments
ID	Location	Proj.	Prop.	Time	ft/sec		
6302	-1		60	1190	2757/2778		Warm up
	-2	160.8	60		2800		Warm up
	-3	160.3	59.5	931	2800		Warm up
	-4	159.5	58	1197	2741/2758		Warm up
	-5	160.7	58	1198	2739/2756		Full penetration apparently caused by very small piece of back face. Spall partial delamination in plate directly above entrance hole. No delamination on sides or bottom.
	-6	160.2	57	1195	2745/2760		Partial Penetration
	-7	160.9	56	1286	2551/2568		Complete delamination of plate. Partial Penetration. Broke off about 1/8 of plate. No visible penetration into titanium.
	-8	160.7	57	1228	2672/2680		Complete plate delamination. (Partial Penetration)
	-9	160.4	57	1250	2625/2634		Partial Penetration No visible delamination.
	-10	160.5	58	1222	2685/2688		Partial Penetration. Plate cracked; delaminated; 3/4 of plate still held at vice clamp area.

Table 2 . Phase II Ballistic Test Results

PLATE #	HARDNESS	STRIKING VELOCITY	RESULTS	COMMENTS	SCALE #	V50 (ft/sec)
20	321/340	793	CP	Impacted on Titanium Surface	326	
20	321/340	737	CP	Impacted on Titanium Surface	327	
20	321/340	637	PP	1mm delamination along top edge	328	
20	321/340	676	CP	Impacted on Titanium Surface	329	
20	321/340	672	CP	Impacted on Titanium Surface	330	
20	321/340	628	CP	Impacted on Titanium Surface	331	
20	321/340	600	PP	Impacted on Titanium Surface	332	
20	321/340	624	PP	Impacted on Titanium Surface	338	2099
20	321/340	623	PP	3mm delamination visible on 4 sides	339	
20	321/340	804	CP	Impacted on steel side	340	
20	321/340	695	PP	Impacted on steel side	341	
20	321/340	746	PP	Impacted on steel side	342	
20	321/340	763	*CP*	Impacted on steel side	343	
20	321/340	762	*PP*	Impacted on steel side	344	2503
21	477/364	771	CP	No apparent delamination	345	
21	477/364	761	CP	.5mm delamination along top edge	346	
21	477/364	718	CP		347	
21	477/364	657	*PP*	2mm delamination along top edge	348	
21	477/364	661	CP		349	
21	477/364	650	*CP*	3mm delamination along top edge	350	
21	477/364	632	*PP*		351	
21	477/364	649	*CP*		352	2122
24	512/364	719	CP		381	
24	512/364	660	*PP*	.5mm delamination along top edge	382	
24	512/364	693	CP		383	
24	512/364	692	CP		384	

24	512/364	664	*CP*		385	
24	512/364	685	CP		386	2172
				Totally delaminated after 6 shots.	386a	
22**	241/340	698	PP	No delamination	387	
22**	241/340	796	*PP*	No delamination	388	
22**	241/340	894	CP	<.5mm delamination	389	
22**	241/340	845	CP		390	
22**	241/340	821	CP	<.5 mm delamination	391	
22**	241/340	787	CP		392	
22**	241/340	767	*CP*	Plate totally delaminated	393	2562
				Totally delaminated after 7 shots.	393a	
23***	512/387	774	PP		394	
23***	512/387	849	CP	Total delamination	395	2660
				Total delamination after 2 shots	395a	
25	555/302	823	*PP*		396	
25	555/302	847	CP		397	
25	555/302	829	*CP*		398	
25	555/302	838	CP	2mm delamination	399	2710
25	555/302	830	CP	Total delamination	400	
				Total delamination after 5 shots	400a	

Additional Notes:
1. Determined from Masciannica, 1981.
2.Perforation of the .5mm 2024 Al witness plate is a CP. *CP* or *PP* results indicate data that were used to calculate the V50 Limit Velocity.
**The zone of mixed results is very large and the number of shots is very small; therefore the V50 should be treated as an approximation. There is also a question of whether performance of the target went down as the plate delaminated.
***This number is a very rough approximation. There are too few shots as a result of the plate delaminating.
Velocity.

Table 3. Explosive Bonding Data Summary

Composite Material	Plate No.	Explosive Bonding Date	Anfo height	Results	Comments	Ti Thickness	Steel Thickness
12" x 12" A2/Ti	1	12/5/97	2.50"	No bonding due to thick coating	Ion plated tantalum coating		
9" x 15" A2/Ti	2	9/12/97	2.50"	Bonded	Ta foil interlayer		
15" x 15" A2/Ti	3	3/3/98	3.00"	80% bonded (180 in.^{2})	4 foil interlayer-	.233	.289
7.5" x 7.5" A2/Ti	4	3/3/98	2.75"	100% bonded	Ion plated tantalum coating	.234	.284
15" x 15" A2/Ti	5	5/27/98	2.50"	100% bonded (56 in.^{2})		.256	.253
15" x 15" D2/Ti	6	5/27/98	2.50"	60% bonded (136 in.^{2})	Pitted titanium	.261	.252
15" x 15" D2/Ti	7	5/27/98	2.50"	70% bonded (157 in.^{2})	Pitted titanium	.257	.251
4" x 8" A2/Ti	8	8/18/98	2.50"	Mostly unknown			
15" x 15" D2/Ti-6-4	9	8/18/98	2.75"	37% bonded (83 in.^{2})		.256	.267
15" x 15" D2/Ti	10	8/17/98	2.50"	90% bonded (202 in.^{2})		.255	.240
15" x 15" A2/Ti-6-4	11	8/18/98	3.00"	90% bonded (202 in.^{2})			
13 ¼" x 13 ¼" D2/Ti-6-4	13	1/20/99	52#	89% bonded (156 in.^{2})		.259	.252
13" x 13" Hi-hard/Ti-6-4	14	1/20/99	55 #	91% bonded (153 in.^{2})	Thick plate	.280	.207
11 ½" x 11"A2/Fe foil/Ti-6-4	15	1/20/99	52 #	16% bonded (20 in.^{2})		.258	.260
11 ½" x 11 ¼"A2/Mo foil/Ti-6-4	16	1/20/99	----	59% bonded (76 in.^{2})		.248	.319
12 ¼" x 12" Hi-hard/Ti-6-4	17	1/21/99	----	95% bonded (139 in.^{2})		.218	.321
13 ½" x 13 ¼" A2/Ti-6-4	18	1/22/99	----	85% bonded (152 in.^{2})		.265	.257
13 ½" x 12" D2/Ti-6-4	19	1/22/99	----	66% bonded (107 in.^{2})		.257	.247
Hi-hard/Ti-6-4	20	5/4/99	50.01#	76% bonded (148 in.^{2})		.217	.257
Hi-hard/Ti-6-4	21	5/4/99	48.89#	79% bonded (154 in.^{2})		.219	.259
Hi-hard/Ti-6-4	22	5/5/99	51.22#	86% bonded (168 in.^{2})		.220	.260
Hi-hard/Ti-6-4	23	5/5/99	51.62#	83% bonded(164 in.^{2})		.227	.260
Hi-hard/Ti-6-4	24	5/5/99	50.17#	84% bonded (165 in.^{2})		.238	.259
Hi-hard/Ti-6-4	25	5/5/99	51.26#	76 % bonded (148.5 in.^{2})		.270	.206

Table 4. Average Microhardness Values of Steel

Fabrication Stage	A2/Ti-6-4	Hi-hard/Ti-6-4
As-received steel material	84 R_b	86 R_b
Explosive bonded plate		22 R_c
Hardened composite plate	62 R_c	46 R_c
Tempered composite plate	62 R_c	46 R_c

Table 5. Average Microhardness Values of Titanium

Fabrication Stage	A2/Ti-6-4	Hi-hard/Ti-6-4
As-received titanium material	31-35 R_c	30 R_c
Explosive bonded plate		33 R_c
Hardened composite plate	31 R_c	34 R_c
Tempered composite plate	38 R_c	33 R_c

Table 6. Bend test results from individual and composite specimens

Composite Material	Quantity	Bend Angle Range	Delamination	Fracture
A2	4	4-27	NA	100% specimens had total fractures.
A2/Ti	5	3-8	80% specimens delaminated	20% specimens had steel fractures.
D2	9	0-14	NA	100% specimens had total fractures.
D2/Ti	2	8-11	None	100% specimens had total fractures.
Hi-hard	11	180	NA	None
Hi-hard/Ti 6 4 hardened	5	1.5-180	75% specimens delaminated	25% specimens had Ti 6 4 fractures.
Hi-hard/Ti 6 4 hardened & tempered	6	11-40	17% specimens delaminated	83% specimens had Ti 6 4 fractures

Table 7. Computer Simulation Results

Armor Type	2500 ft/sec bullet velocity	2700 ft/sec bullet velocity	2800 ft/sec bullet velocity	3000 ft/sec bullet velocity
.089" Ti .098" S7 Steel			Full penetration of bullet.	
.250" A2 Steel .225" Ti			Bullet does not penetrate steel.	
.250" Steel .225" titanium	Bullet plugs in titanium layer	Bullet lodges in composite, and a plug of material is released.		
.175" A2 steel .275" titanium	Bullet breaks through titanium layer and a small plug of material is removed.	Bullet lodges in composite, and a plug of material is released.		
.275" A2 steel .175" titanium	Bullet is stopped prior to titanium layer	Bullet lodges in composite, and a plug of material is released.		
.060" titanium .190" A2 steel .200" titanium	Bullet breaks through thin outer titanium and steel layer and lodges in titanium layer	Bullet lodges in composite, and a plug of material is released.		
.060" titanium (20% stronger yield strength) .190" A2 steel .200" titanium		Bullet lodges in composite, and a plug of material is released.		
.060" titanium (20% weaker) .190" A2 steel .200" titanium		Bullet lodges in composite, and a plug of material is released.		
.060" TiB2 .190" A2 Steel .200" Ti-6-4		Bullet does not penetrate thin TiB2 coating.		Bullet does not penetrate thin TiB2 coating.

Table 8. Quantitative impact test results as illustrated in Figure 3

Pt.	1	2	3
Load at Point (lb)	4109.4	6243.15	7002.57
Energy at Point (ft-lbs)	6.40	28.11	72.11

Table 9

Lambda Research, Inc.

7512.d01 STRESS40.17 12/17/97

RESIDUAL STRESS DEPTH ANALYSIS

With Stress Gradient and Relaxation Corrections
and Diffraction Peak Width (B 1/2)

STEEL/TITANIUM SANDWICH SAMPLE LONGITUDINAL DIRECTION
Sample 9 Titanium Side

E/(1+ν)= 13154. +- 210. ksi 1/2 S2 = 11.02 +- .18 x 10-6 1/MPa
MU= 2320. 1/in. (91.3 1/mm) Sectioning Stress Relax. = .0 ksi

	DEPTH in.	(mm)	RESIDUAL STRESS ksi (MPa) Measured		Gradient		Relaxation		B 1/2 (deg)
1	.00000	(.0000)	1.9± .6	(13.± 4.)	2.6	(18.)	2.6	(18.)	1.18
2	.00260	(.0660)	-.2± .5	(-1.± 4.)	.0	(0.)	.0	(0.)	.99
3	.00520	(.1321)	1.2± .6	(8.± 4.)	1.0	(7.)	1.0	(7.)	1.02
4	.01100	(.2794)	12.7± .8	(87.± 5.)	12.5	(86.)	12.1	(84.)	1.08
5	.01990	(.5055)	8.5± .7	(59.± 5.)	8.6	(59.)	7.3	(50.)	1.12
6	.04830	(1.2268)	-13.9± .9	(-96.± 5.)	-13.8	(-95.)	-14.2	(-98.)	1.08
7	.10100	(2.5654)	-19.0± .9	(-131.± 6.)	-19.0	(-131.)	-10.1	(-70.)	1.15
8	.14820	(3.7643)	-20.9± 1.0	(-144.± 7.)	-20.9	(-144.)	-3.4	(-23.)	1.24
9	.19970	(5.0724)	-21.1± 1.0	(-146.± 7.)	-21.1	(-146.)	5.6	(39.)	1.32
10	.24000	(6.0960)	-16.4± 1.0	(-113.± 7.)	-16.4	(-113.)	14.5	(100.)	1.38

Table 10

Lambda Research, Inc.

7512.d02 STRESS40.17 12/16/97

RESIDUAL STRESS DEPTH ANALYSIS

With Stress Gradient and Relaxation Corrections
and Diffraction Peak Width (B 1/2)

STEEL/TITANIUM SANDWICH SAMPLE LONGITUDINAL DIRECTION
Sample 10 Steel Side

E/(1+ν)= 26716. +- 267. ksi 1/2 S2 = 5.43 +- .05 x 10-6 1/MPa
MU= 2244. 1/in. (88.3 1/mm) Sectioning Stress Relax. = .0 ksi

	DEPTH in.	(mm)	RESIDUAL STRESS ksi (MPa) Measured		Gradient		Relaxation		B 1/2 (deg)
1	.00000	(.0000)	59.2± 1.8	(408.± 12.)	59.9	(413.)	59.9	(413.)	1.99
2	.01000	(.2540)	26.4± 1.4	(182.± 10.)	26.9	(185.)	23.1	(160.)	2.33
3	.01900	(.4826)	4.3± 1.1	(30.± 8.)	4.7	(32.)	-.2	(-1.)	2.11
4	.04900	(1.2446)	-3.2± 1.0	(-22.± 7.)	-3.2	(-22.)	-6.7	(-46.)	1.88
5	.09900	(2.5146)	-12.4± 1.1	(-86.± 8.)	-12.4	(-86.)	-11.4	(-79.)	1.75
6	.15000	(3.8100)	-25.8± 1.2	(-178.± 8.)	-25.7	(-178.)	-14.2	(-98.)	1.63
7	.20300	(5.1562)	-40.5± 1.3	(-279.± 9.)	-40.5	(-279.)	-9.0	(-62.)	1.58

Table 11. Actual Chemical Composition of Titanium and Steel Plates

Element	Titanium, Grade 2	Ti-6-4	A-2 Tool Steel	D2 Tool Steel	Hi-hard steel
Iron	.04-.10	.12-.22	Remainder	Remainder	Remainder
Oxygen	.12-.16	.090-.19			
Nitrogen	.004-.006	.007-.011			
Carbon	.01-.02	.010-.02	.95-1.05	1.4-1.6	.30
Hydrogen	13/14 ppm	.0010-.0092			
Copper					.033
Titanium	Rem. (See note 1)	Rem.			.044
Zirconium					.002
Tin					.002
Silicon			.50 max.	.5 max.	.27
Manganese			.45-.90	.5 max.	1.39
Sulfur			.03 max	.03 max.	.003
Phosphorous			.03 max.	.03 max.	.011
Tungsten					
Boron					.0005
Columbian					.002
Chromium			4.75-5.50	11-13	.044
Vanadium		3.79-4.23	.15-.50	.15-1.10	.004
Aluminum		5.915-6.41			
Nickel					.026
Molybdenum			.90-1.40	.70-1.20	.27
Cobalt					
Beta Transus		1781-1822°F	NA	NA	NA

Table 12. Mechanical Properties of As-Received Titanium and Ti-6-4 Material

	Titanium, Grade 2	Ti-6-4
Tensile Strength (transverse) (psi)	61,500/71,600	138,000-151,000
Tensile Strength (longitudinal)	62,500-71,000	136,000-159,000
Yield Strength @ .2% offset (psi)(transverse)	41,400-54,400	132,000-148,800
Yield Strength @ .2% offset (psi)(longitudinal)	46600-50,200	124,300-154,000
Elongation (%)transverse	24-28	12-16
Elongation (%)longitudinal	26-29	11-17

Table 13. Composite Plates Submitted for Ballistic Testing

Plate No.	Stress relief temperature	Hardening Temperature and Time	Tempering Temperature and Time	Comments
20	1050°F for 4 hours	1600°F for 70 sec. (edge)	350°F for 1 hour	
21	1050°F for 4 hours	1600°F for 300 sec. (edge)	350°F for 1 hour	
22	1050°F for 4 hours	1560°F for 320 sec. (center)	400°F for 1 hour	
23	1050°F for 4 hours	1630°F for 320 sec. (center)	400°F for 1 hour	Plate was straightened
24	1050°F for 4 hours	1568°F for 300 sec. (center)	400°F for 1 hour	Plate was straightened
25	1050°F for 4 hours	1600°F for 300 sec. (center)	400°F for 1 hour	.020" thick fused coating

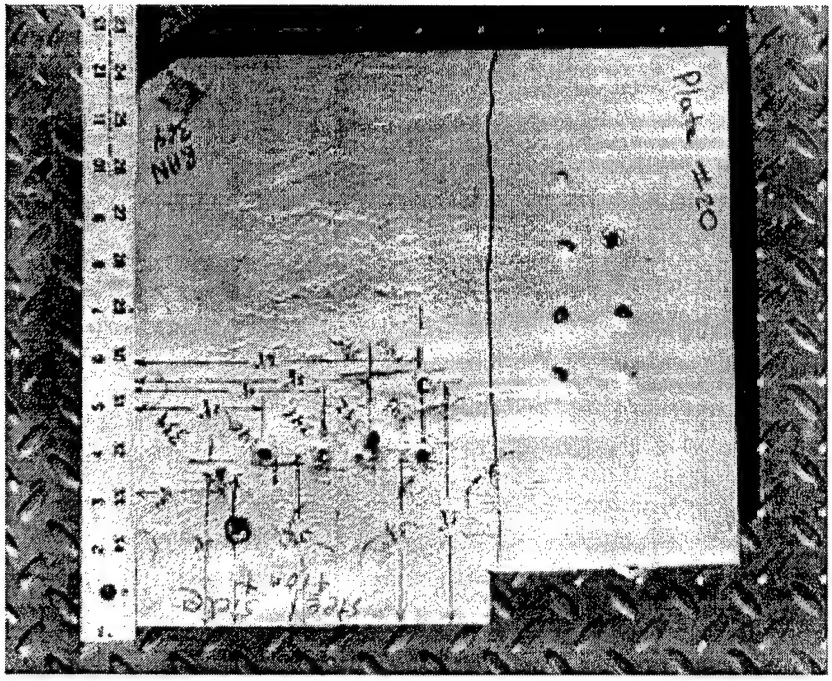

Photo 1. Plate 20. Steel side up showing location of ballistic tests. Plate was struck14 timesV50 data was 2099 ft/sec.

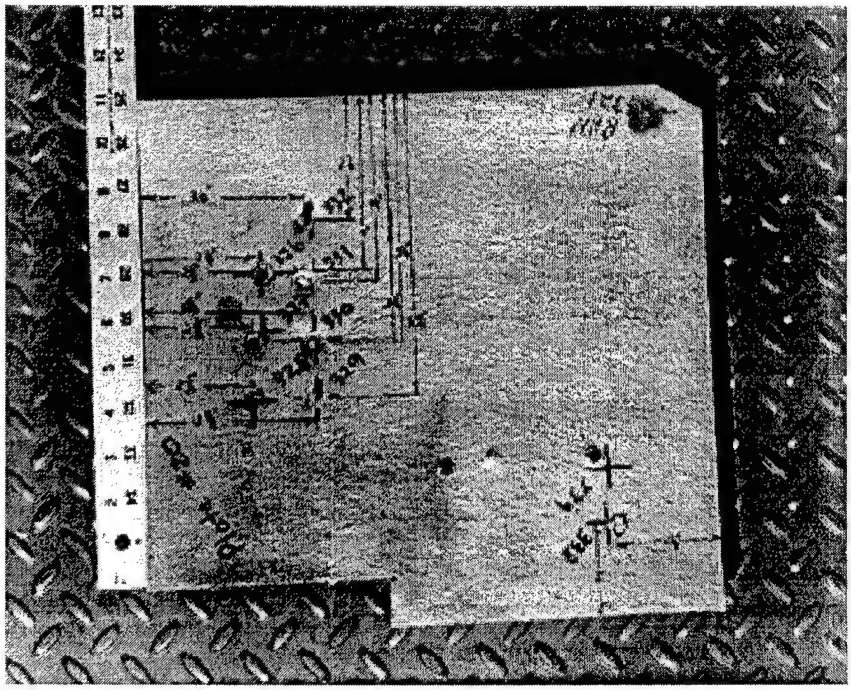

Photo 2. Plate 20. Titanium side up showing location of ballistic tests. Plate was struck14 times. V50 data was 2099 ft/sec.

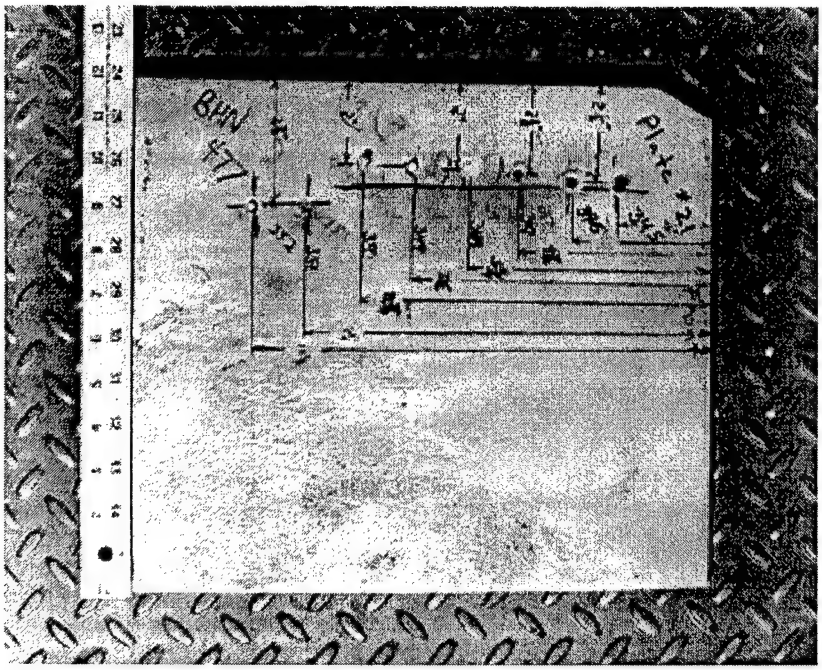

Photo 3. Plate 21. Steel side up showing location of ballistic tests. Note that all tests are along one edge. Plate was struck 8 times. V50 data was 2503 ft/sec.

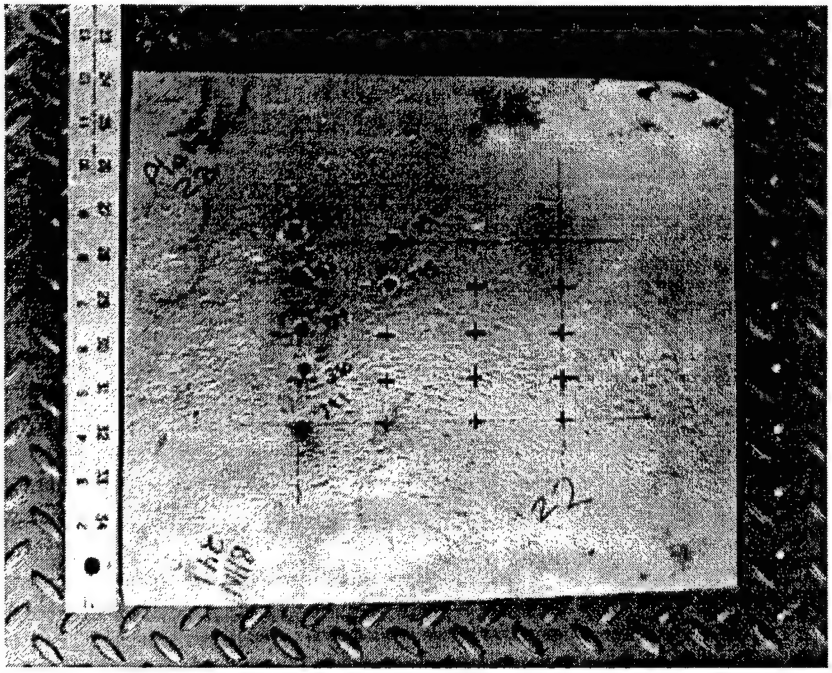

Photo 4. Plate 22. Steel side up. Note that ballistic test is in the center of the plate. Plate was struck 7 timesV50 data was 2562 ft/sec.

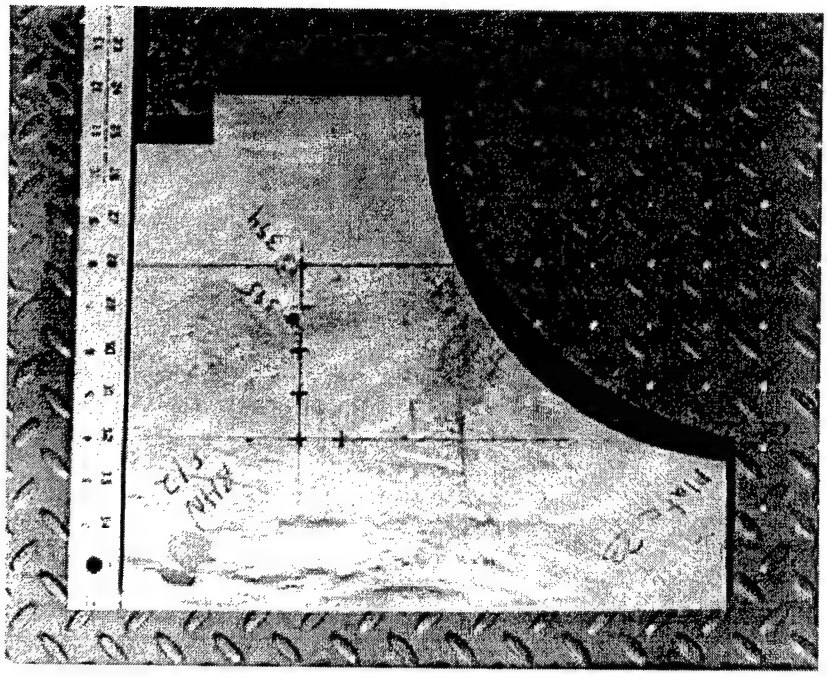

Photo 5. Plate 23. Steel side up. Plate was straightened after tempering. Plate was struck 2 times. V50 data was 2660 ft/sec.

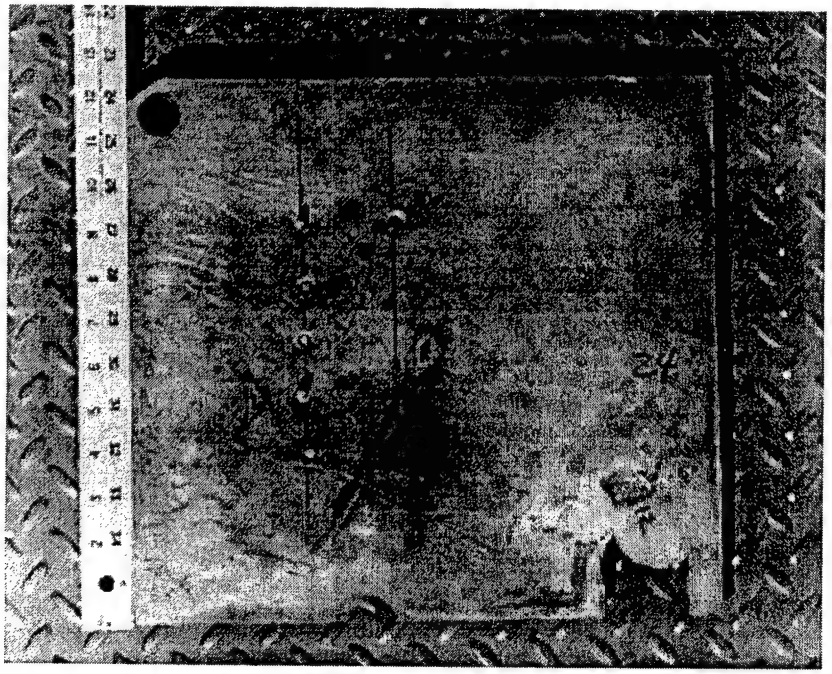

Photo 6. Plate 24. Steel side up. Plate was straightened after tempering. Plate was struck 6 times.V50 data was 2172 ft/sec.

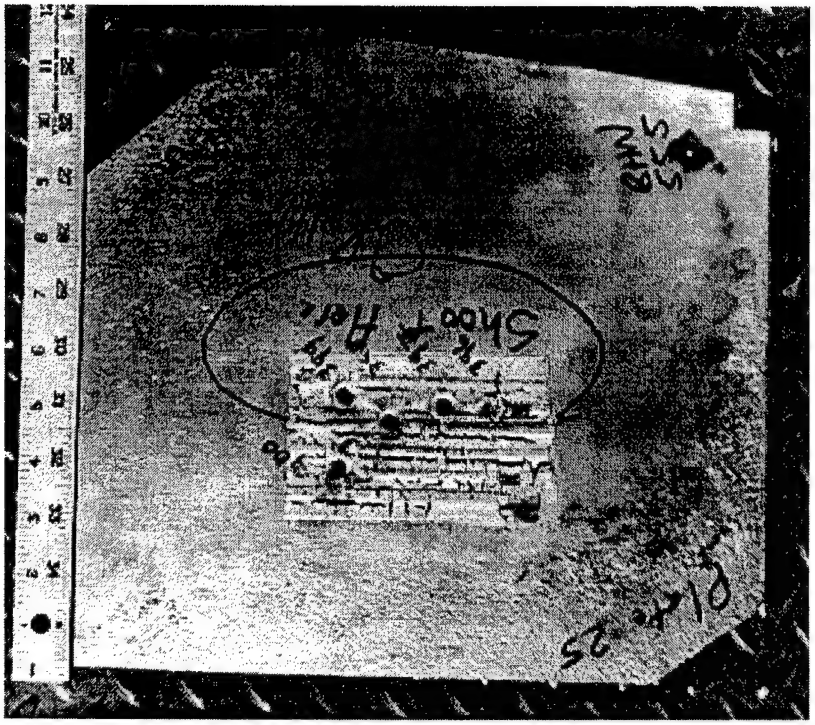

Photo 7. Plate 25. Steel side up. Ballistic testing conducted in center of plate in the area of the 60Rc hardened coating. Plate was struck 5 times. V50 data was 2710 ft/sec.

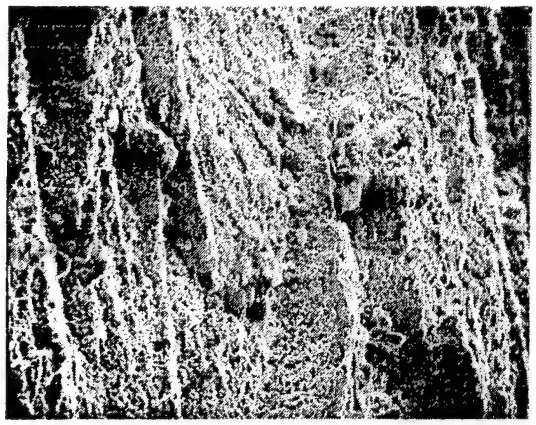

Photo 8. SEM photo exhibiting a brittle area of Titanium material at 500X magnification near the joint interface.

Photo 9. SEM photo showing ductile area of the titaniummaterial at 2500X magnification

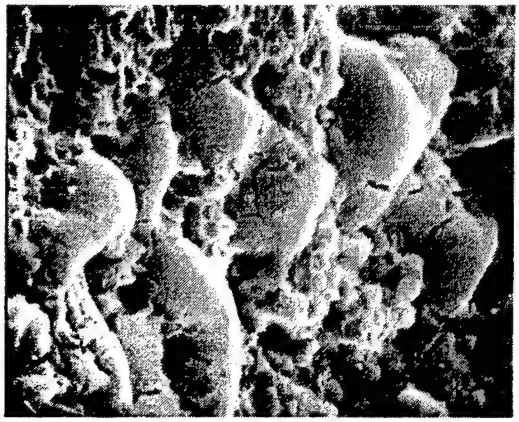

Photo 10. SEM photo at 5000X magnification within the steel illustrating brittle platelets with transgranular cracks surrounded by a ductile matrix near the leading edge of the ballistically damaged region.

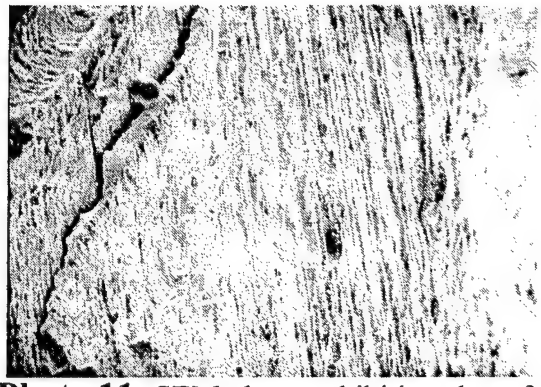

Photo 11. SEM photo exhibiting shear fracture at 50X magnification within the steel.

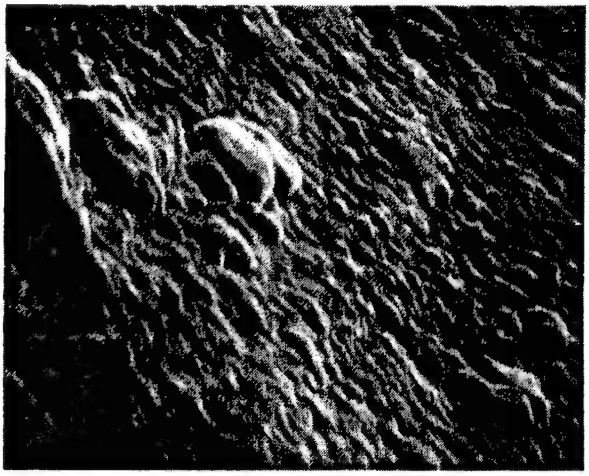

Photo 12. SEM photo at 15,000X magnification showing the tantalum ion plated interface.

Photo 13. Sem photo at 200X showing brittle intermetallic layer of brass.

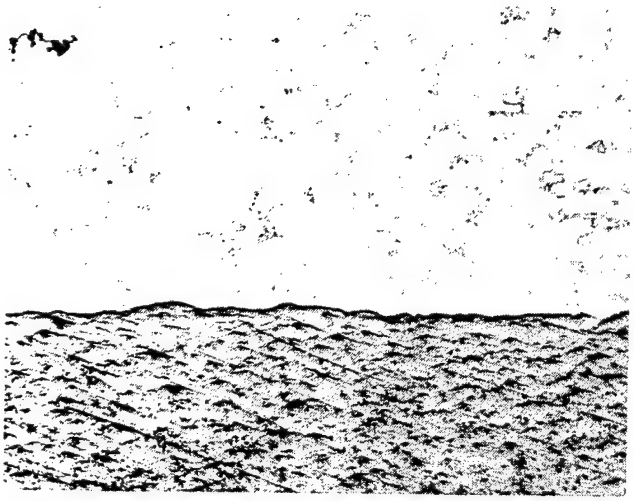

Photo 14. Photomicrograph showing a smooth or waveless interface.

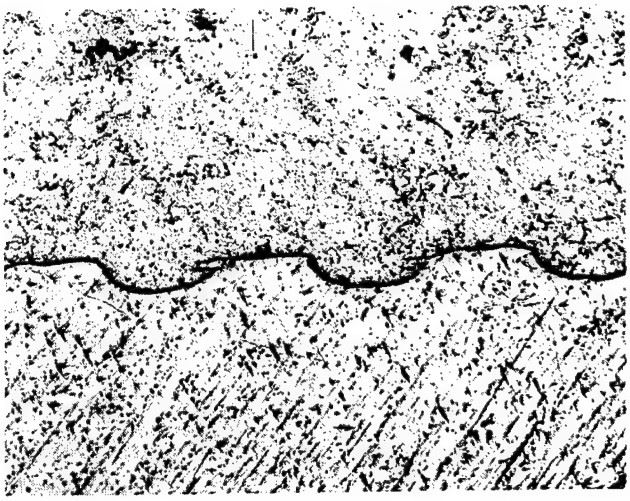

Photo 15. Photomicrograph showing large asymmetrical waves.

Photo 16. Photomicrograph showing fine, symmetric wavy interface.

Photo 17. Photomicrograph showing large symmetrical waves.

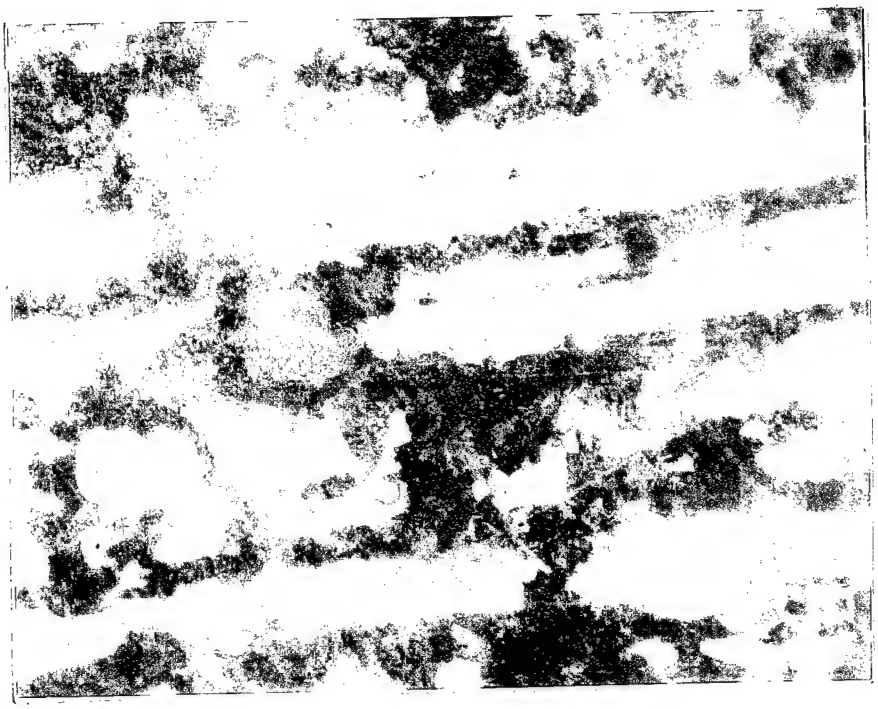

Photo 18. As-received Hi-hard material (#1131) at 400X magnification, exhibits a banded arrangement of ferrite and pearlite. Etched with 2% nital.

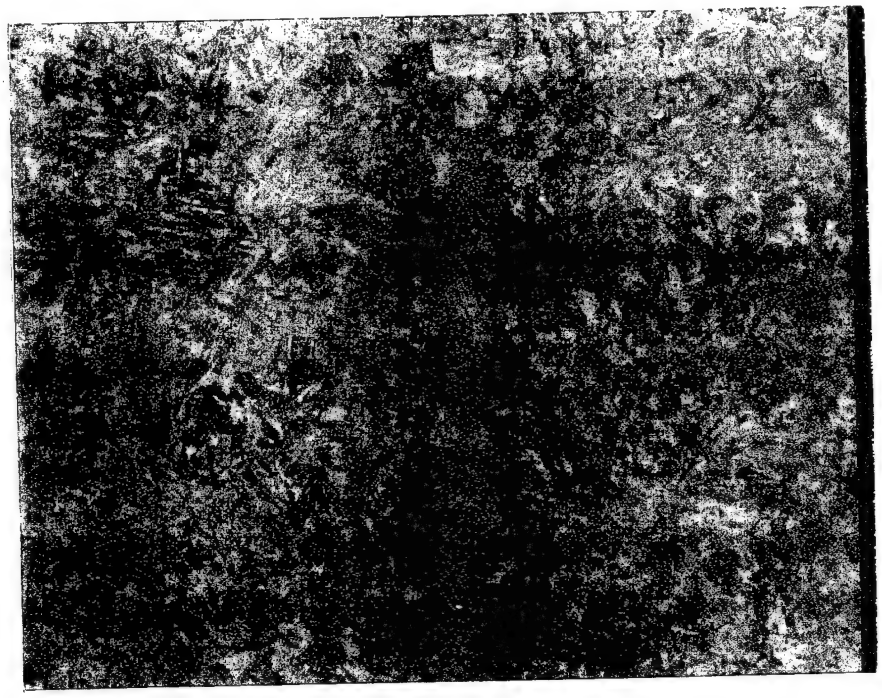

Photo 19. Hardened Hi-hard material showing a martensitic structure (#1136) at 500X magnification. Etched with 2% nital.

Photo 20. Hardened and tempered Hi-hard (#1134) at 500X magnification presents a tempered martensitic structure. Etched with 2% nital.

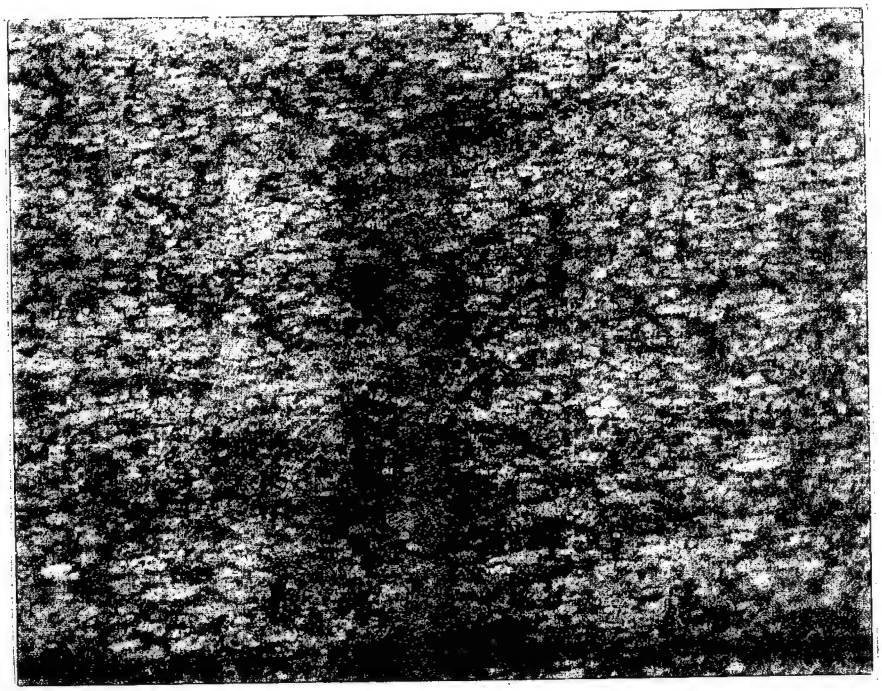

Photo 21. As-received Ti-6-4 material illuminates a lamellar Titanium structure at 200X magnification (#1139). Etched with Krolls reagent.

Photo 22. Hardened Hi-hard/Ti-6-4 illustrated (#1126) at 200X magnification showing the brittle intermetallic region at the interface. Etched with 2% nital.

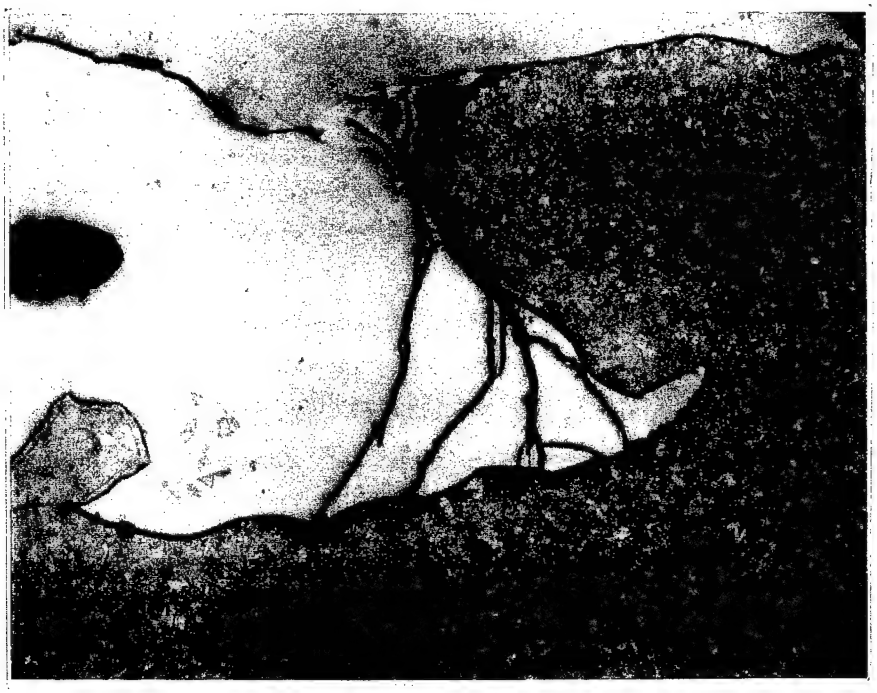

Photo 23. Hardened and tempered Hi-hard/Ti-6-4 (#1137) at 200X magnification. Notice the carbide particles in the brittle region. Etched with 2% nital.

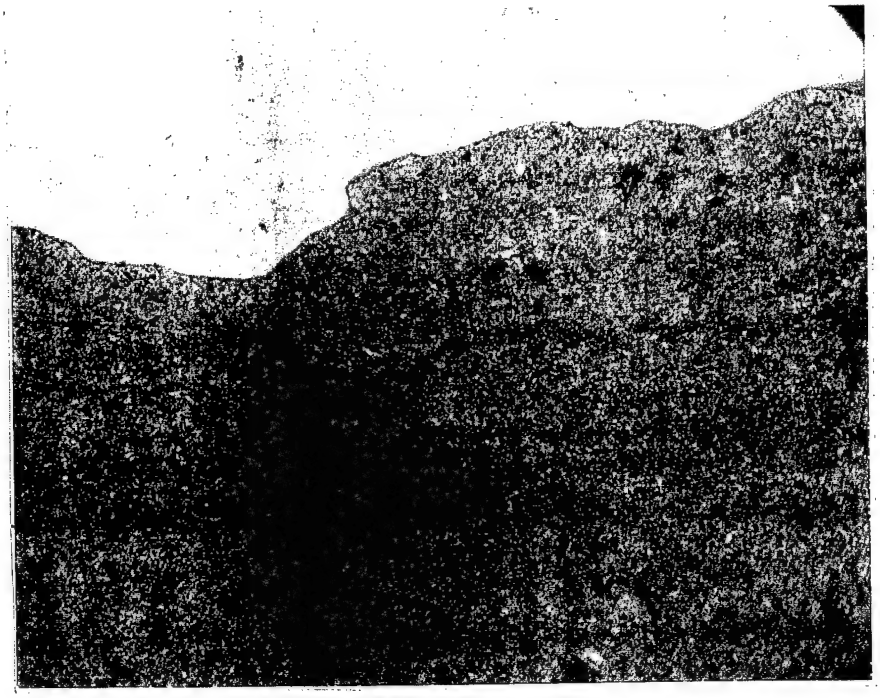

Photo 24. Hardened A2/Ti composite specimens showing the joint interfacial region with 150 angstrom thick layer of tantalum. Note that no cracks or noticeable intermetallic region exists.

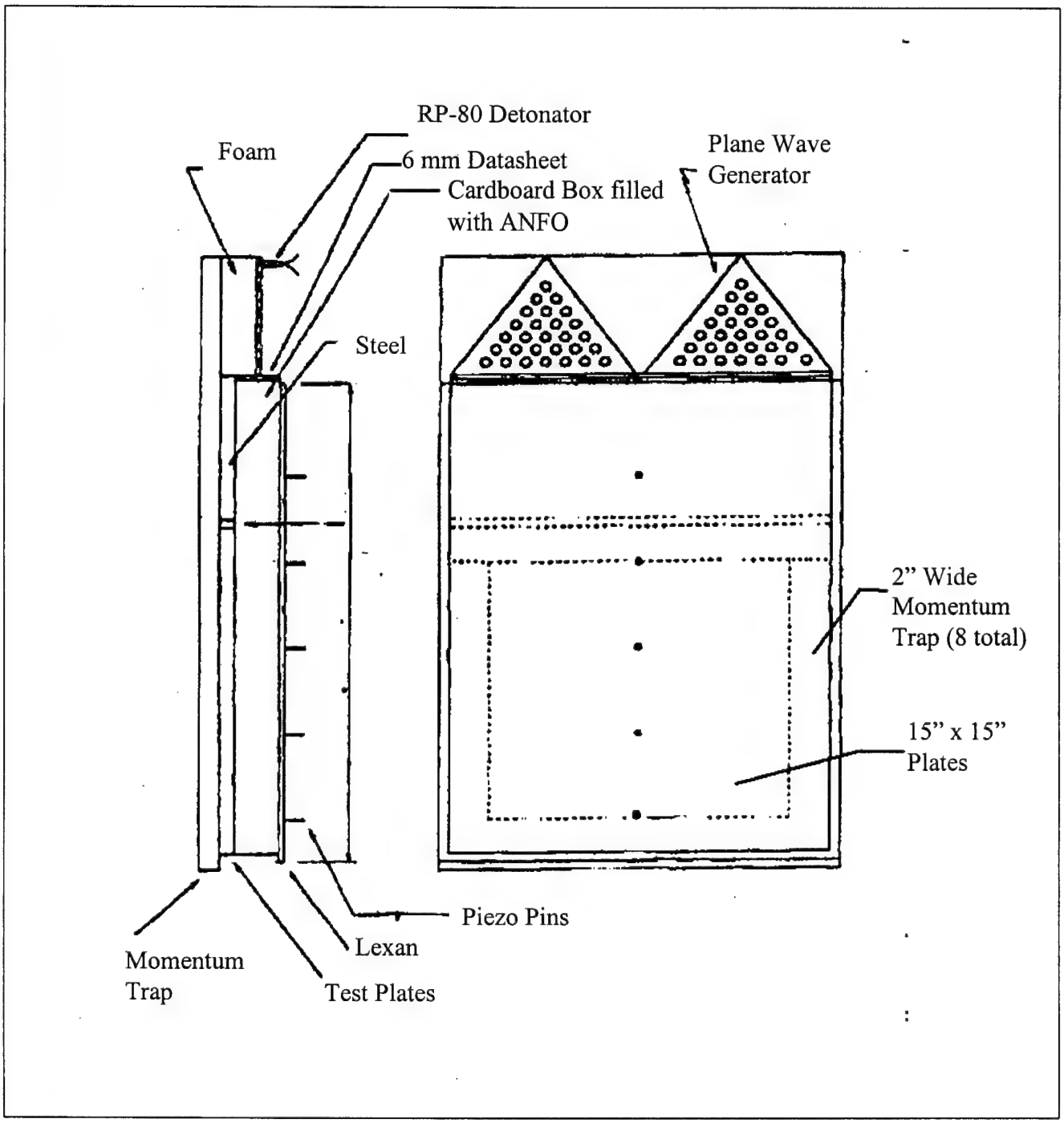

FIGURE 1

Explosive Welding Setup

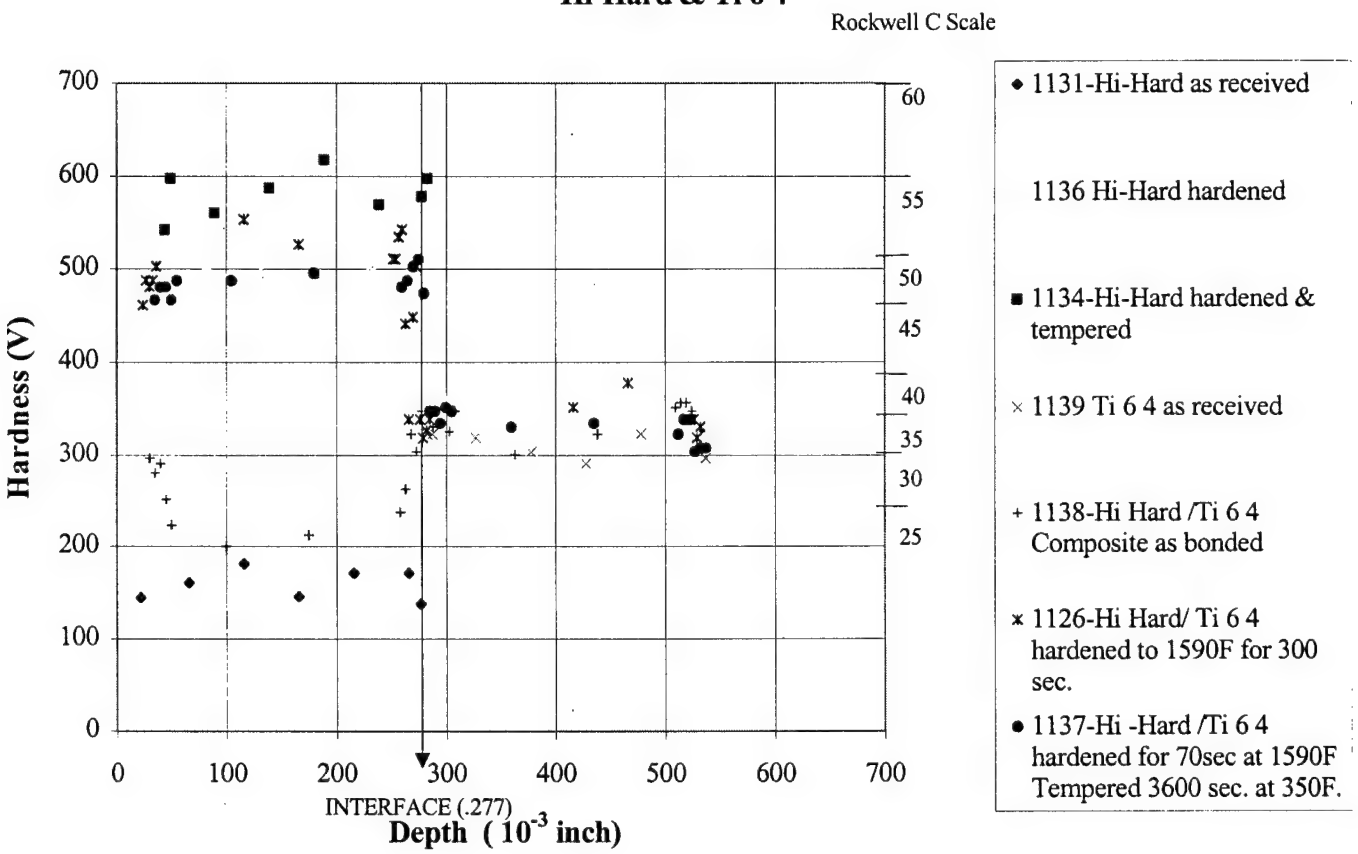

FIGURE 2

TYPICAL CHANGE IN COMPOSITE HARDNESS AS A FUNCTION OF THE PROCESSING.

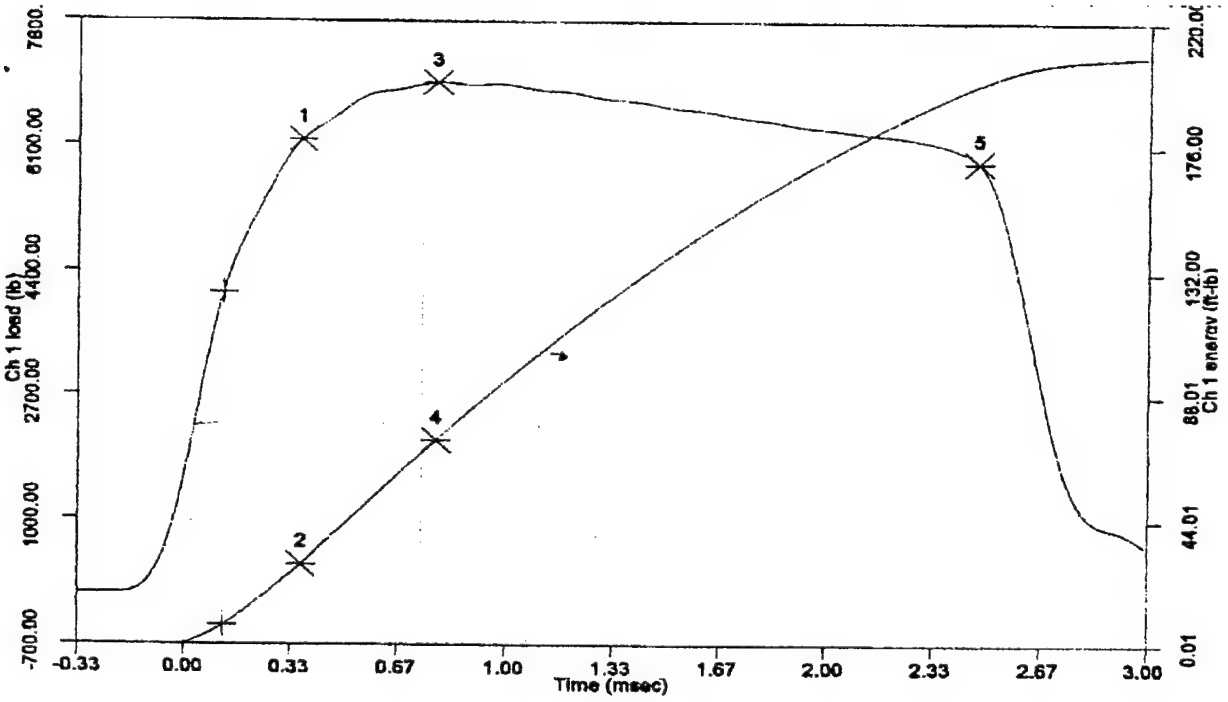

FIGURE 3

DYNATUP IMPACT TEST RESULTS OF FIVE A2/TI AS-BONDED

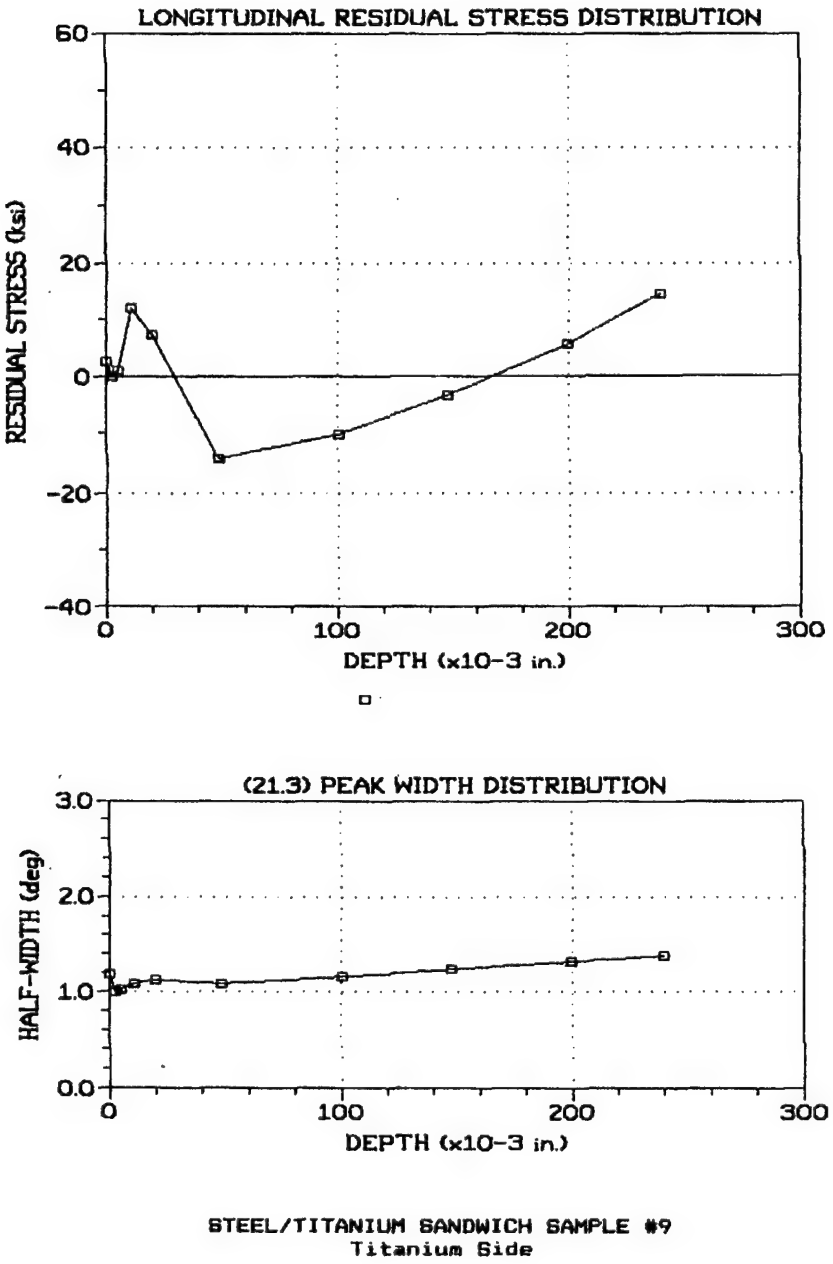

FIGURE 4

RESIDUAL STRESS TEST DATA FOR THE TITANIUM SIDE OF AN A2/TI COMPOSITE.

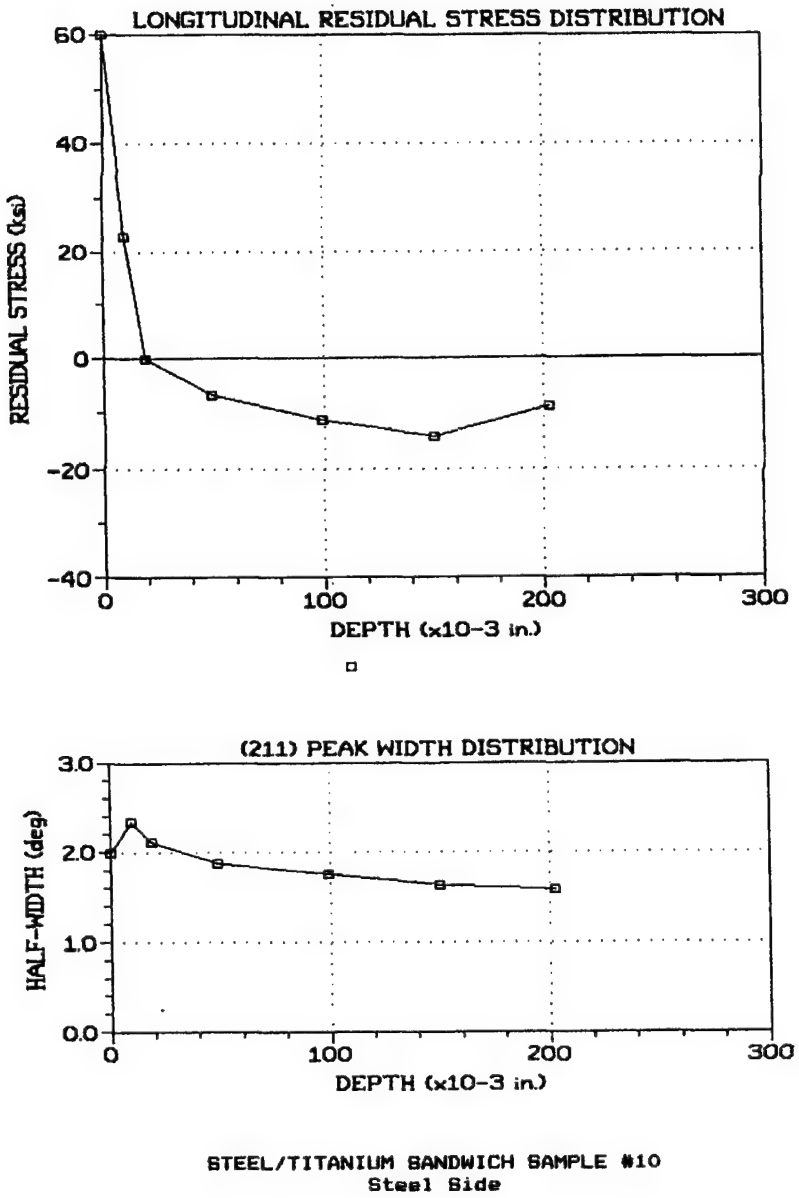

5

FIGURE 5

RESIDUAL STRESS DATA FOR THE STEEL SIDE OF AN A2/TI COMPOSITE.

Hi-Hard Hardness/BendAngle vs. Soak Temp. at a Soak Time of 60-70 sec.

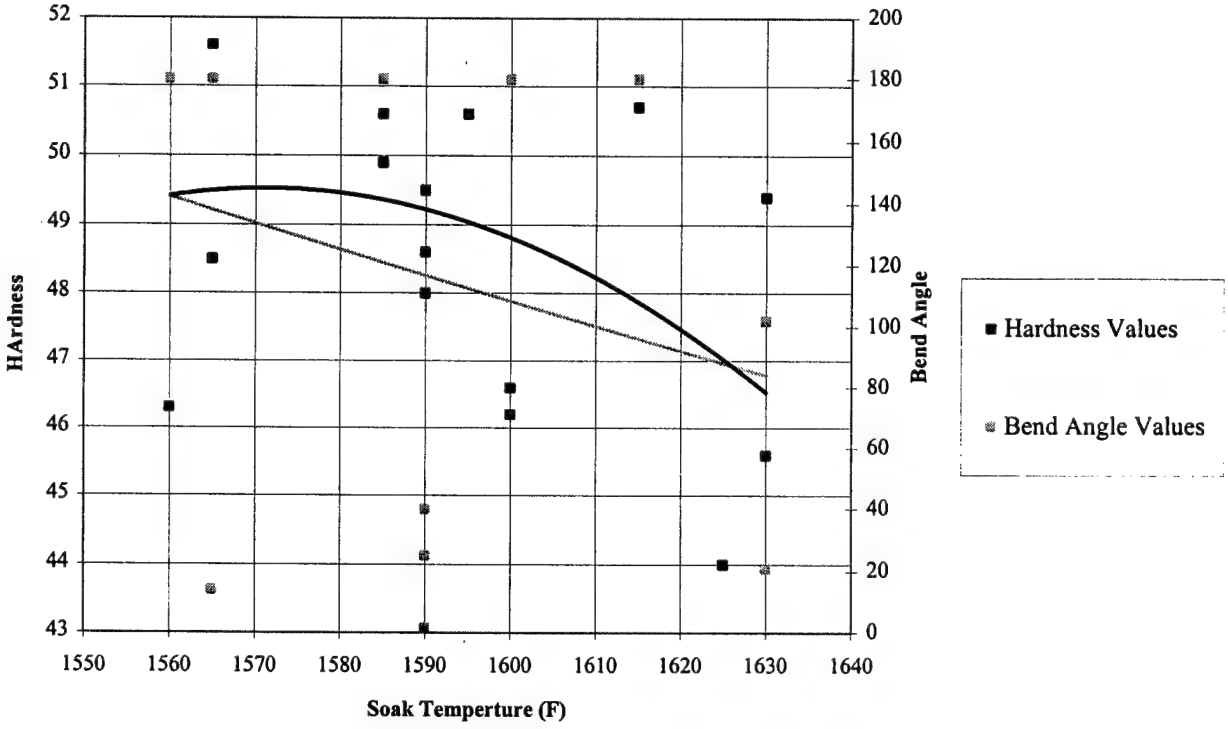

Figure 6.1

A2 Hardnes/Bend Angle Data vs. Soak Temp at a Soak Time of 600 sec.

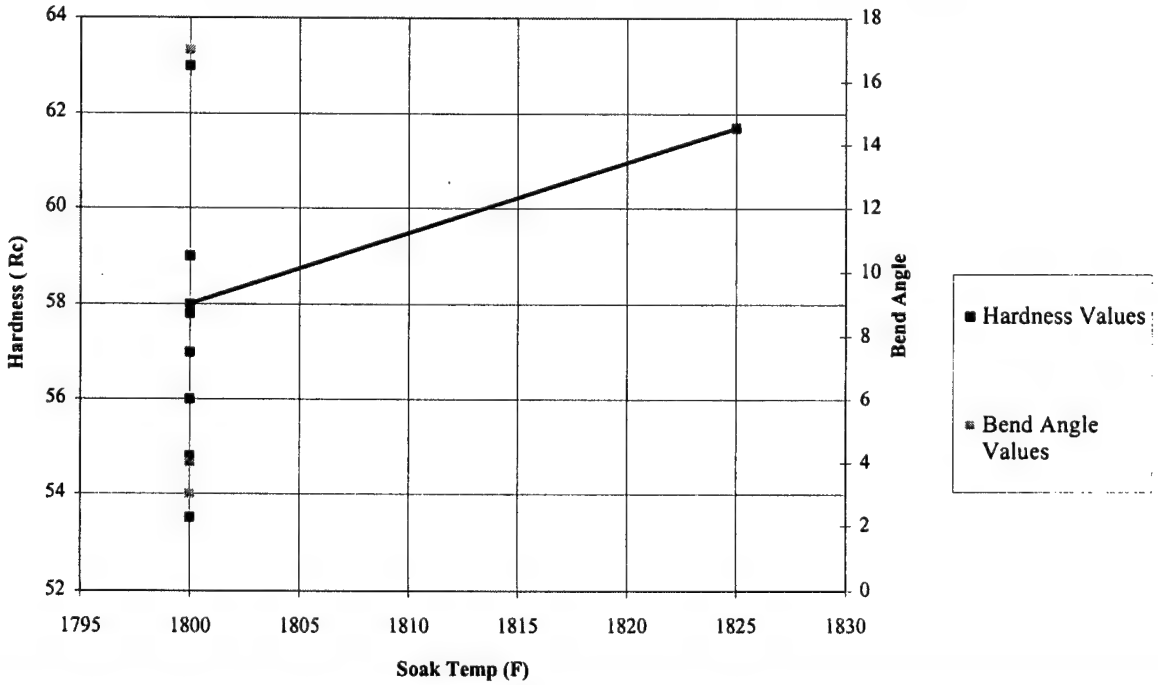

Figure 6.2

Hi-Hard Hardness/Bend Angle vs.Soak Time at Soak Temp of 1585-1630 F

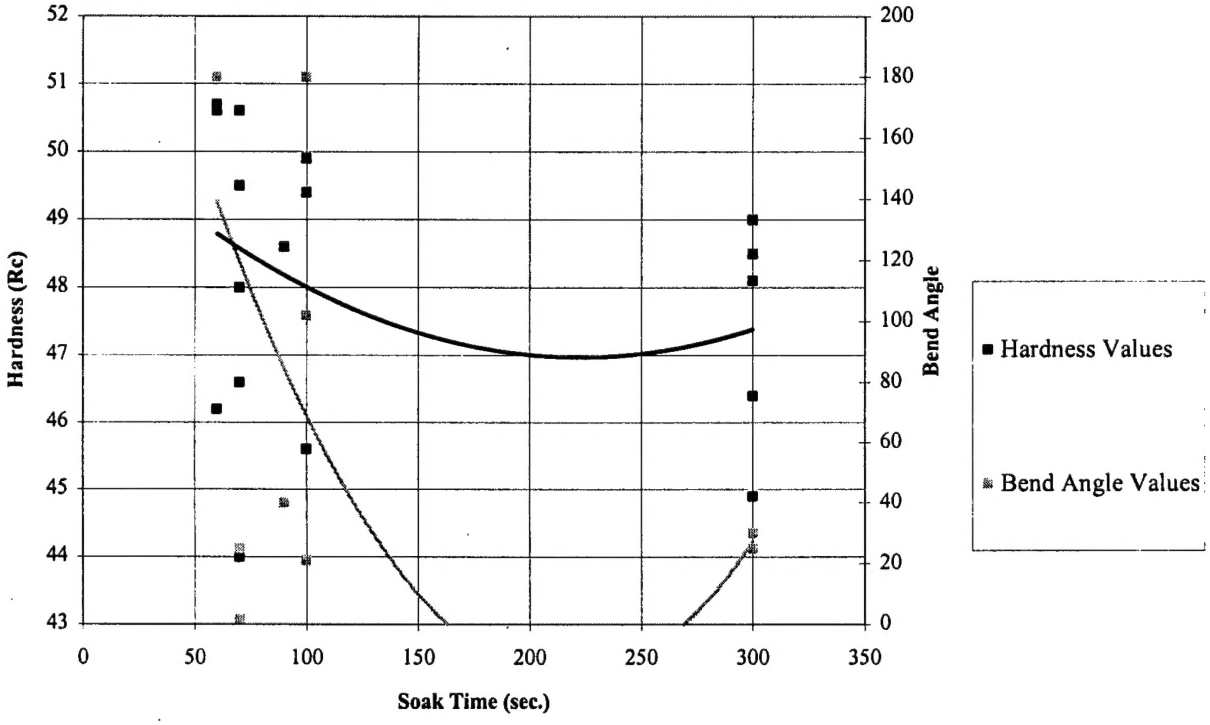

Figure 7.1

A2 Hardness/Bend Angle vs. Soak Time at a Soak Temp. of 1800 F

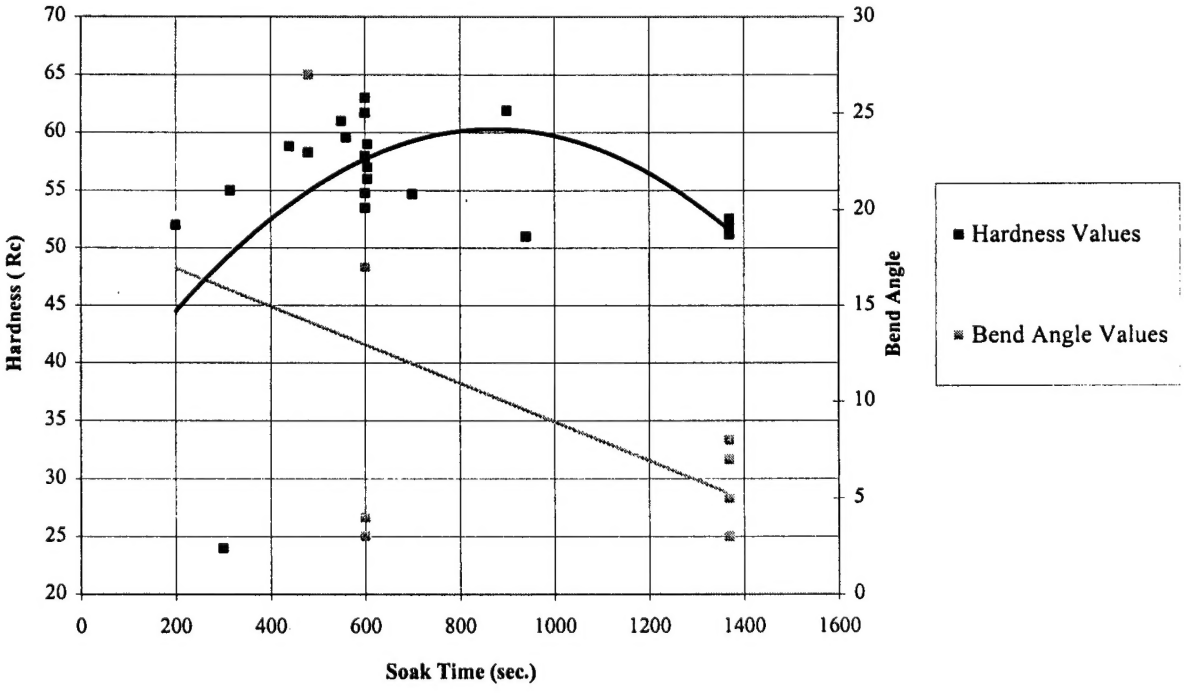

Figure 7.2

Hi -Hard Hardness/Bend Angle vs. Tempering Temp. at a Soak Temp. of 1560 1630 F and a Soak Time of 60-100 sec.

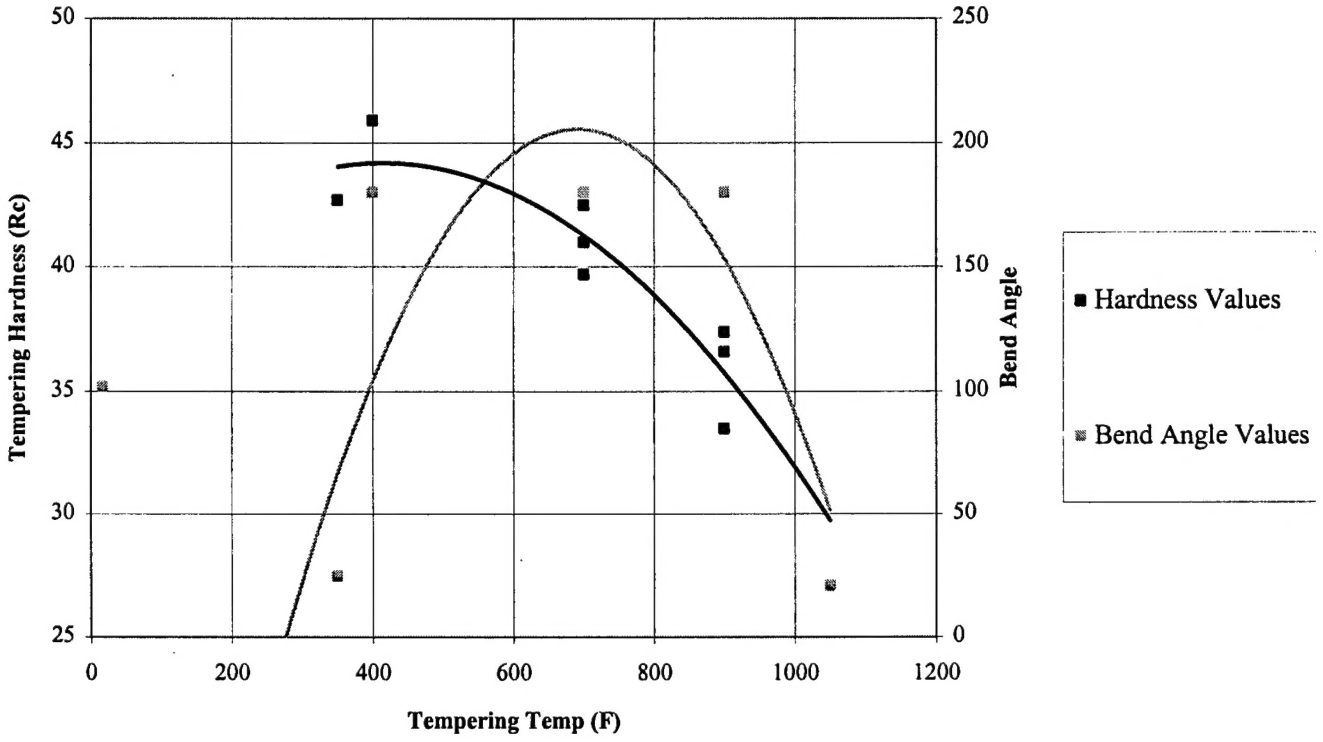

Figure 8.1

A2 Hardness/Bend Angle Data vs. Thermal Gradiant at a Soak Temp. of 1800 F

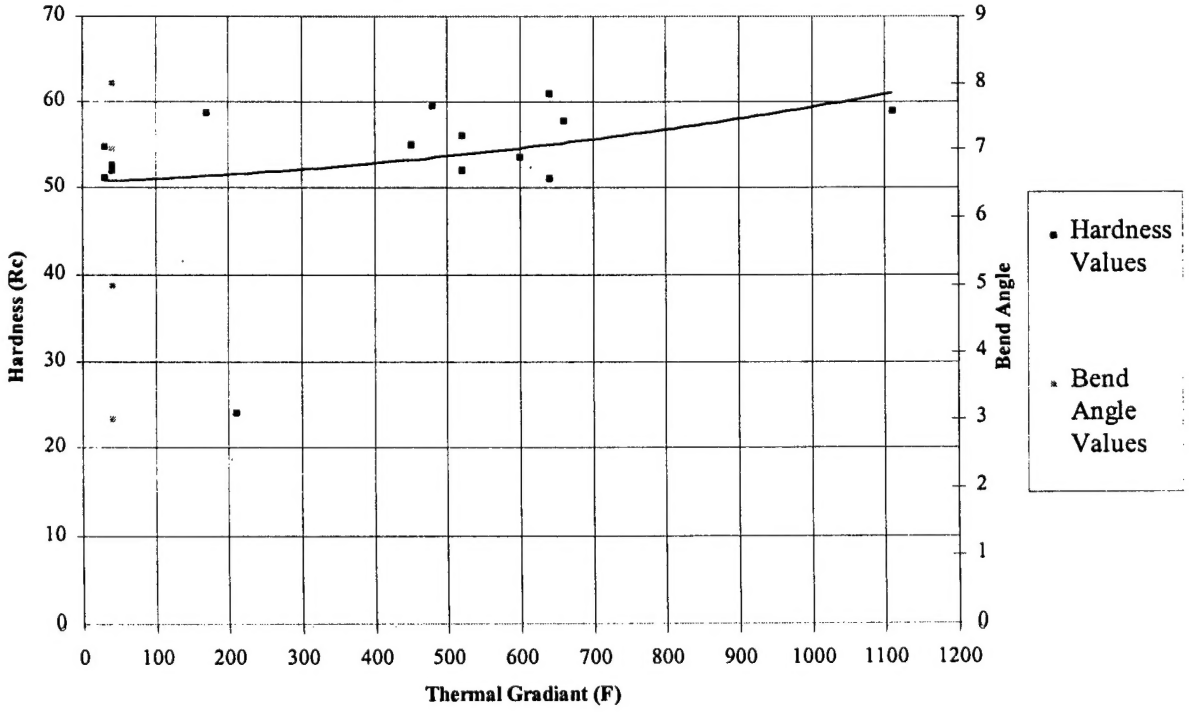

Figure 8.2

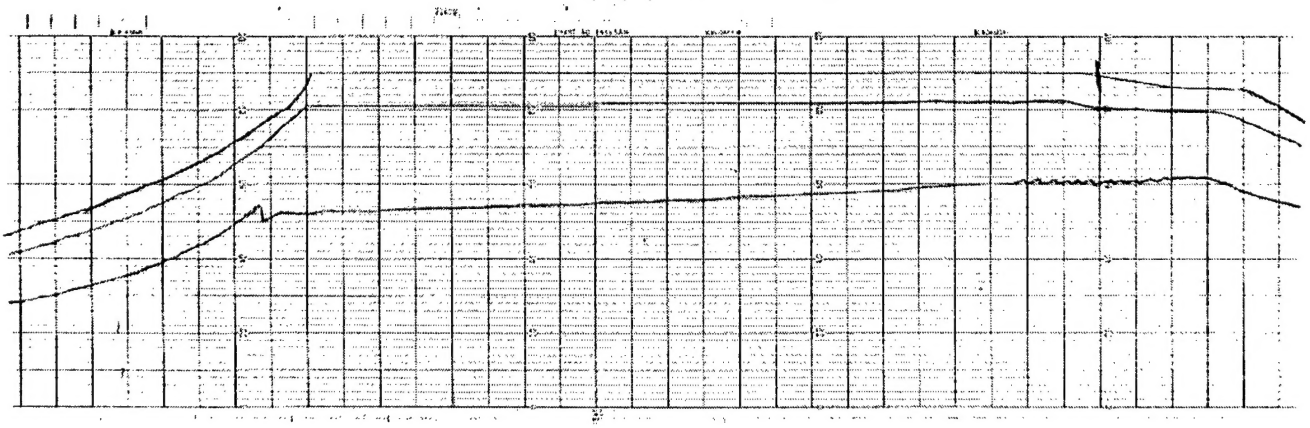

Figure 9

CHART OF THERMAL GRADIENT BETWEEN THE TITANIUM SURFACE, INTERFACE AND STEEL SURFACE. THE X-AXIS MEASURES TIME AND THE Y-AXIS MEASURES TEMPERATURE IN FAHRENHEIT WITH THE MAXIMUM VALUE REPRESTING 2000°F. THE HIGHEST TEMPERATURE RECORDED IS AT 1800°F REPRESTING THE STEEL SURFACE TEMPERATURE. THE INTERFACE IS AT 1640°AND THE TITANIUM SURFACE TEMPERATURE IS AT 1200°F FOR A TOTAL THERMAL GRADIENT OF 600°F.

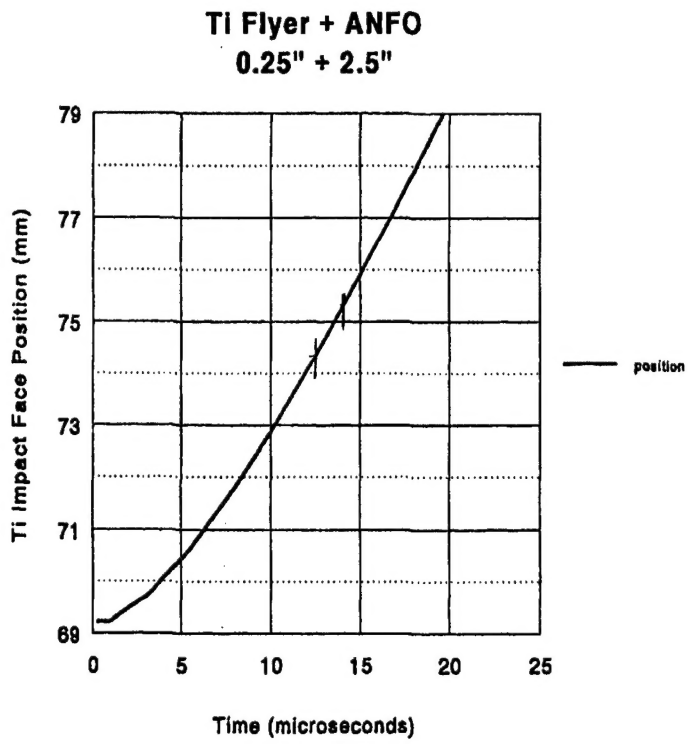

FIGURE 10

CALCULATED FLYER PLATE POSITION AT VARIOUS TIMES WITH AMMONIUM NITRATE/FUEL OIL MIXTURE.

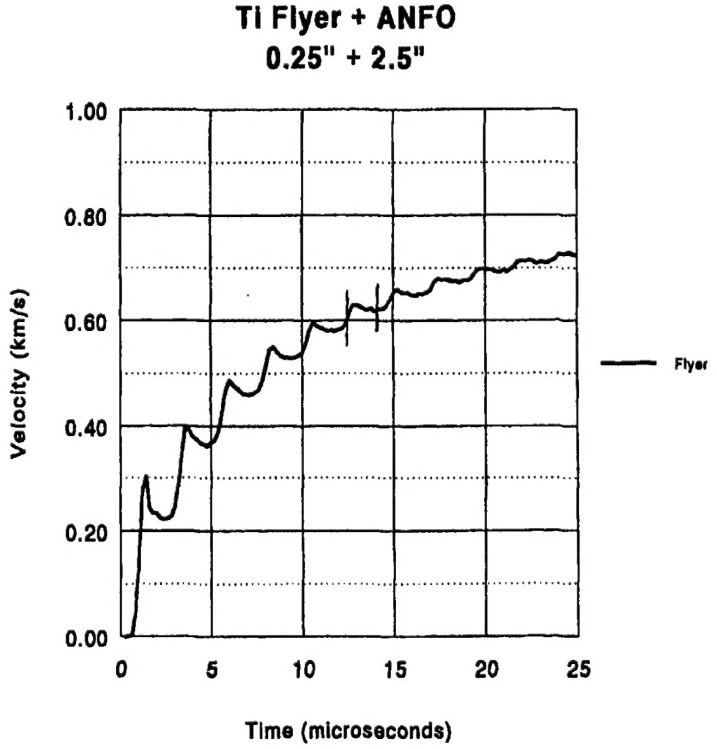

FIGURE 11

CALCULATED TITANIUM IMPACT FACE POSITION AT VARIOUS TIMES WITH AMMONIUM NITRATE/FUEL OIL.